



Departamento de Física
Universidade de Coimbra

Cardioaccelerometry

The assessment of Pulse Wave Velocity using
Accelerometers

Project Report
5th year
Graduation in Biomedical Engineering

Helena Catarina de Bastos Marques Pereira

Setembro de 2007





Faculdade de Ciências e Tecnologia
da Universidade de Coimbra



Faculdade de Medicina
da Universidade de Coimbra

This report is made in fulfillment of the requirements of **Project**, a discipline of the 5th year of the Biomedical Engineering graduation.

Supervisors	Prof. Dr. Carlos M. Correia Prof. Dr. Luís Requicha Ferreira Physics Department FCTUC	
External Supervisor	João Maldonado, MD Instituto de Investigação e Formação Cardiovascular	

*“...Pedras no caminho?
Guardo todas, um dia vou construir um castelo...”*

ABSTRACT

In the past recent years, great emphasis has been placed on the role of arterial stiffness in the development of cardiovascular diseases, recognized as the leading cause of death in the world. This hemodynamic parameter, generally associated to age and blood pressure increase, can be assessed by the measurement of the pulse wave velocity (PWV), i.e., the velocity at which the pressure wave propagates along an artery. Although PWV measurement is accepted as the most simple, non-invasive, robust and reproducible method to determine arterial stiffness over the carotid-femoral region, the devices available in the market for this purpose are extremely expensive.

This research project aims at developing alternative instrumental methods for the aortic PWV's hemodynamic characterization and, at a later stage, a software application for acquisition and interpretation of this information. The proposed instruments are constituted by one accelerometric probe and a multisensor acquisition module, which includes classic electrodes of electrocardiography, piezoelectric (PZ) transducers and, foreseen, one pressure sensor.

Up to now, in its research usage, it has proved effective in the prolonged follow up of hypertensive patients without and with drug treatment, allowing the study of correlations between the different types of signals. A valuable contribution to this study has been given by the bench models developed in laboratory for the ADXL203 accelerometer calibration and pulsatory system simulation.

This report describes not only the aspects related with the overall instrument architecture, the successive developed versions and the results obtained, under medical control, for each of the input signals, but also the calibration and pulsatory models and respective results.

Keywords: Cardiovascular Diseases, Aortic Stiffness, Pulse Wave Velocity, Accelerometer based Probe, Multisensor Acquisition Module, Clinical Research Tests.

RESUMO

Nos últimos anos, tem sido dada grande ênfase ao papel da rigidez arterial no desenvolvimento de doenças cardiovasculares, reconhecidas como a principal causa de morte mundial. Este parâmetro hemodinâmico, associado normalmente ao aumento da idade e da pressão arterial, pode ser avaliado pela medição da velocidade de onda de pulso (VOP), ou seja, a velocidade com que a onda de pressão se propaga ao longo de uma artéria. Embora a medição da VOP seja aceite como o método mais simples, não-invasivo, robusto e reprodutível para determinar a rigidez arterial ao longo da região carótida-femoral, os equipamentos disponíveis no mercado para este efeito são extremamente dispendiosos.

Este projecto de investigação pretende desenvolver métodos instrumentais alternativos para a caracterização hemodinâmica da VOP aórtica e, numa fase mais avançada, uma aplicação informática que permita a aquisição e a interpretação dessa informação. Os instrumentos propostos são constituídos por uma ponta de prova acelerométrica e um módulo de aquisição multisensor, que incorpora eléctrodos clássicos de electrocardiografia, transdutores piezoeléctricos e, como previsão, um sensor de pressão.

Até agora, o seu uso em testes clínicos, provou ser eficaz no seguimento prolongado de pacientes hipertensivos sem e com tratamento de fármacos, permitindo o estudo de correlações entre os diferentes tipos de sinais. Para este estudo contribuíram ainda os modelos de bancada desenvolvidos em laboratório, com vista à calibração do acelerómetro ADXL203 e à simulação de um sistema pulsatório.

Neste relatório são descritos não só os aspectos ligados à arquitectura do instrumento, as sucessivas versões desenvolvidas e os resultados obtidos, sob supervisão médica, para cada um dos canais de informação, mas também, os modelos de calibração e pulsatório e, respectivos resultados.

Palavras-chave: *Doenças Cardiovasculares, Rigidez Arterial, Velocidade de Onda de Pulso, Ponta de Prova Acelerométrica, Módulo de Aquisição Multisensor, Testes Clínicos.*

ACKNOWLEDGEMENTS

This academic project has been a great personal learning experience and I would like to thank everyone who helped me throughout this year.

First and foremost, I am very grateful to my supervisors, Prof. Dr. Carlos Correia and Prof. Dr. Requicha Ferreira by their continuous guidance, support, assistance and friendship. Prof. Dr. Carlos Correia is the author of this project idea and was a great counsellor throughout my graduation. Prof. Dr. Requicha Ferreira, due to his technical expertise and creative mind, was essential in this project fulfilment.

Special thanks go to the other member of this team: Dr. João Maldonado, who supervised all clinic tests and without his medical knowledge and helpful discussions this work would not have been possible. Thanks to the staff that work at Instituto de Investigação e Formação Cardiovascular for their invaluable collaboration and sympathy.

The Centro de Electrónica e Instrumentação has a great environment and I must thank all for the kindness and availability, not forgetting for sure my work colleagues, Ana and Edite, for their group effort.

I would like to express my gratitude also to Eng^o Augusto, who gave an important assistance, as far as the mechanical part of this project is concerned.

My deepest thanks go to my parents, brothers and friends for their constant support and encouragement. They have always allowed me to keep my mental and physical shape throughout my studies, particularly one person, Paulo, who always has been there.

CONTENTS

Abstract	vi
Resumo	vii
Acknowledgments	ix
List of Figures	xiii
List of Tables	xv
1. Introduction	1
1.1 Motivation	1
1.2 Objectives.....	2
1.3 Hemodynamic project team.....	3
1.4 Overview of the report.....	4
2. Theoretical Background	4
2.1 Arterial Stiffness and Pulse Wave Velocity.....	4
2.1.1 General Concepts.....	4
2.1.2 PWV Measurement	5
2.1.2.1 State of the art	6
2.2 Accelerometric Sensors	8
2.2.1 Introduction.....	8
2.2.2 General Concepts.....	8
2.3 Electrocardiography.....	11
2.3.1 Introduction.....	11
2.3.2 Components of the ECG	12
2.3.3 Instrumentation Requirements.....	13
3. Process Methodology	17
3.1 Introduction.....	17
3.2. Measurement System Architecture.....	17
3.3 Clinical Trials	19
3.3.1 Data Acquisition.....	19
3.2.2 Data Processing.....	19
3.4 Discussion.....	21
4. Measurement Probes	23
4.1 Introduction.....	23

4.2 Spring-Loaded Probe	24
4.3 Differential Probe.....	25
4.4 Hybrid Probe	27
5. Acquisition Modules.....	29
5.1 Introduction.....	29
5.2 Module A	29
5.3 Module B	30
5.4 Module C.....	31
5.5 Module D	32
5.6 Module E.....	33
6. Accelerometer Calibration.....	34
6.1 Introduction.....	34
6.1.1 Slider Crank Mechanism.....	34
6.2 Methods	36
6.2.1 Experimental Configuration	36
6.2.2 Experimental Measurements.....	37
6.3 Results and Discussion.....	37
6.3.1 Experience A	37
6.3.2 Experience B	38
6.4 Conclusions	40
7. Pulsatory model.....	42
7.1 Bench Model Set-up.....	42
7.2 Results.....	43
7.3 Data Processing.....	43
8. Clinical Research Tests.....	46
8.1 CTs Procedures.....	46
8.2 Data Pre-Processing	47
9. Conclusions and future work.....	51
9.1 Conclusions.....	51
9.2 Future Work	52
Appendices.....	53
Appendix A	53
Appendix B	57

LIST OF FIGURES

Figure 1 Measurement of PWV with the foot-to foot method.....	6
Figure 2 Complior®.....	6
Figure 3 Sphymocor®	6
Figure 4 The basic spring mass system accelerometer	9
Figure 5 Flip Calibration.....	10
Figure 6 Form of a normal ECG signal	12
Figure 7 Cardiac Cycle Diagram.....	12
Figure 8 Heart’s electrical activity.....	13
Figure 9 Typical single-channel electrocardiograph.....	15
Figure 10 General measurement system architecture.....	18
Figure 11 NI USB-6008©.....	18
Figure 12 Developed Instrument.....	19
Figure 13 Original Signals of a young and healthy subject, obtained with the accelerometer based instrument and visualized in Matlab®.....	20
Figure 14 Overlap of eight selected peaks and mean of these overlapped peaks.....	21
Figure 15 Pulse wave Contour in some arteries.....	22
Figure 16 SLP	24
Figure 17 Schematic of the forces applied on the SLP during data acquisition.....	25
Figure 18 DP.....	26
Figure 19 Hybrid Probe.	28
Figure 21 DAQ Module B.....	30
Figure 22 Block Diagram of the linear power supply design.....	31
Figure 23 DAQ Module C.....	32
Figure 24 DAQ Module D.....	32
Figure 25 DAQ Module E.....	33
Figure 26 Crank Mechanism	35
Figure 27 Graphic representation of the piston movement (blue) and MHS (red).....	36
Figure 28 Experimental set-up of accelerometer calibration.....	36
Figure 29 Data Pre Processing.....	39
Figure 30 Accelerometer’s Curve Calibration	40

Figure 31 Set-up of the developed bench model.....	42
Figure 32 Accelerometric, PZ and pressure signals acquired in the pulsatory model.....	44
Figure 33 Accelerometric and Double Differentiate PZ Signals.....	45
Figure 34 Signals acquired by the SLP/Module B in one patient.....	47
Figure 35 Signals acquired by the SLP/Module C in one patient.....	48
Figure 36 Signals acquired by the DP/Module D in one patient.....	49
Figure 37 Functions of a piezoelectric sensor.....	53
Figure 38 The Heart.....	54
Figure 39 Location of the precordial leads.....	55
Figure 40 Location of the electrodes in the Standard Limb Leads and Augmented Limb leads.....	55
Figure 41 ECG components: waves, segments and intervals.....	56
Figure 42 Measurement probe's circuit schematic.....	57
Figure 43 PZ Single Channel of DAQ Module B.....	57
Figure 44 PZ channel of DAQ Module C.....	58
Figure 45 SPL Electronic Circuit Schematic.....	59
Figure 46 HP Electronic Circuit Schematic.....	60
Figure 47 Electrocardiograph Electronic Circuit Schematic.....	61

LIST OF TABLES

Table 1 Team members of the project 'Hemodynamic Parameters - New Instrumentation and Methodologies' and its contributions.....	2
Table 2 Clinical conditions associated with increased arterial stiffness.....	5
Table 3 Types of ECG leads.....	11
Table 4 Some NI USB-6008 Specifications	18
Table 5 Summary of the developed modules and its main features.....	33
Table 6 Comparison between piston motion and SMH equations.....	35
Table 7 Amplitude, peak voltage and peak acceleration values.....	39
Table 8 Acquisition types performed with the various probes/modules.....	46

CHAPTER 1

INTRODUCTION

1.1 Motivation

Cardiovascular diseases (CVDs) are the leading cause of death in the world. According to the World Health Organization, 17.5 million people died from CVDs in 2005 (30% of all global deaths) and in 2015 is expected that this number rises to 20 million^[1] ^[2].

Recent studies demonstrated that arterial stiffness is a marker of cardiovascular (CV) risk and aortic stiffness holds a strong predictive potential, as intermediate endpoint for CV events ^[3].

Arterial stiffness, which increases with age, hypertension and other factors, can be assessed by the measurement of the pulse wave velocity (PWV), i.e., the velocity at which the pressure wave propagates along an artery.

PWV measurement is universally accepted as the most simple, non-invasive, robust and reproducible method to determine arterial stiffness, and is usually evaluated over the carotid-femoral region. In fact, the aortic PWV measurement is considered as the 'gold-standard' since aorta and its first branches are responsible for most of the pathophysiological effects of arterial stiffness ^[3-6].

At present, several commercial devices are available, that provide automated measurement of aortic PWV. The two systems in common use are the Complior® (Colson) and the Sphygmocor® (AtCor), based in piezoelectric (PZ) sensors and arterial tonometry, respectively ^[7]. Although these devices are based in different sensor technologies, they are both extremely expensive.

Thus a sensor capable of evaluating aortic PWV and elastic properties of the arterial wall accurately and, furthermore, if it can be low-priced, has great potential in this medical field ^[8].

Accelerometer sensors based equipments have several advantages compared to the other presented types: they are inexpensive and can deliver 1, 2 or 3 measurement-axes. In addition, the accelerometers provide a large bandwidth (DC to a few kilohertz) which allows to them to acquire a huge amount of information. These benefits make this type of equipment interesting for measuring different parameters of the pulse wave.

1.2 Objectives

The objectives of this project are to develop alternative instrumental methods, based in accelerometry, for the PWV's hemodynamic characterization and, at a later stage, also a software application for acquisition and interpretation of this information. Both the developed instrumental prototypes and the application must be conceived for use by staff technicians in a clinical environment.

1.3 Hemodynamic project team

This project was carried out in the Centro de Electrónica e Instrumentação da Universidade de Coimbra (CEI) in the framework of a partnership with Instituto de Investigação e Formação Cardiovascular (IIFC). It is a part of the research project 'Hemodynamic Parameters - New Instrumentation and Methodologies', which aims the development of instrumental methods (prototypes and computer applications) for the assessment of blood perfusion in microcirculation and pulse wave velocity.

The work team involved in this global project and its contributions are summarized in Table 1.

Table 1 Team members of the project 'Hemodynamic Parameters - New Instrumentation and Methodologies' and its contributions.

Team Members	Main Contribution		Institution
Prof. Dr. Carlos Correia	Scientific and Technical Supervisors	General Software Development	CEI
Prof. Dr. Requicha Ferreira		General Hardware Development	
Dr. João Maldonado	Clinical Supervisor	Clinical Research Trials/Prototypes validation	IIFC
Catarina Pereira	Biomedical Engineering Project Students	Assessment of PWV	Departamento de Física da Universidade de Coimbra
Ana Ferreira		Assessment of Blood Perfusion in Microcirculation	
Edite Figueiras			

A webpage was also created, and an entire project's information is available on <http://victoria.fis.uc.pt/ppessoais/hemo2006/>.

1.4 Overview of the report

The remaining of this report is organized as follows: Chapter 2 presents a brief overview of the arterial stiffness role in hemodynamic evaluation and the importance of PWV measurement. A theoretical background of accelerometers and electrocardiography is also given.

Chapter 3 contains general information about the instrument architecture and the work done previously by this group in the field of cardioaccelerometry. Chapters 4 and 5 focus in instrumentation developed for clinical data acquisition. Therefore, all the versions of measurement probes and acquisition modules are explained.

Chapters 6 and 7 describe the experimental set-up for the accelerometer calibration and the pulsatory model, respectively. The results obtained in both the systems are interpreted.

Chapter 8 depicts the procedures of the clinical trials and establishes a comparison between the data acquired with the various developed instruments.

Finally, Chapter 9 draws conclusions, summarizes this report and addresses a few suggestions for future work.

The appendices complete the theoretical themes and contain further details on the various technical aspects of the developed instrumentation.

References

- [1] Xu, Minnan., "Local Measurement of the Pulse Wave Velocity using Doppler Ultrasound." Master's Thesis, Massachusetts Institute of Technology, 2002
- [2] 'WHO| Cardiovascular diseases', WHO-World Health Organization, Feb 2007, World Health Organization. 15 Jul 2007. <http://www.who.int/mediacentre/factsheets/fs317/en/index.html>
- [3] Laurent, S. et al, "Expert consensus document on arterial stiffness: methodological issues and clinical applications", Special article, *European Heart Journal*, 27, pp. 2588-2605, Sep.2006
- [4] Nichols, W.W. and O'Rourke, M.F., *McDonald's Blood Flow in Arteries: Theoretical, Experimental and Clinical Principles*, 5th ed. London: Hodder Arnold, 2005, pp. 63-72
- [5] Safar, M. et al, "Aortic Pulse Wave Velocity: an Independent Marker of Cardiovascular Risk", *J Geriatr Cardiol*, 11, pp.295-298, 2002
- [6] Blacher, J. et al, "Aortic Pulse Wave Velocity as a Marker of Cardiovascular Risk in Hypertensive Patients", *Hypertension*, 33, pp.1111-1117, 1999
- [7] Milasseau, Sandrine et al, "Evaluation of Carotid-Femoral Pulse Wave Velocity: Influence of Timing Algorithm and Heart Rate ", *Hypertension*, 45, pp.222-226, 2005
- [8] Hast, Jukka., "Self-mixing interferometry and its applications in noninvasive pulse detection". Master's Thesis, University of Oulu, 2003

CHAPTER 2

THEORETICAL BACKGROUND

This chapter begins with an overview of the arterial stiffness role in hemodynamic evaluation and the importance of PWV measurement. Later, section 2.3 describes in a few words, the basic principles of accelerometers used during the development of our instrumental prototypes. The last section, more extensive, is dedicated to electrocardiography, which was incorporated on the acquisition modules as the main time reference.

2.1 Arterial Stiffness and Pulse Wave Velocity

2.1.1 General Concepts

I. Wave propagation in an elastic tube

An artery is a viscoelastic tube whose diameter varies with a pulsating pressure; in addition, it will propagate pressure and flow waves, generated by the ejection of blood from the left ventricle, at a certain velocity, which is largely determined by the elastic properties of the arterial wall [1].

The relationship between PWV (velocity at which the pressure wave propagates along the artery) and the elasticity of a thin-walled tube filled with an incompressible fluid is expressed by the Moens-Korteweg Equation [2]:

$$PWV = \sqrt{(Eh/2R\rho)} \quad \text{(Eq.1)}$$

From this equation, it is seen that the PWV (m/s) is related to the square root Young's modulus of elasticity (E), where h represents the wall thickness, r the radius and ρ the density of fluid.

Therefore measuring the PWV leads an estimate of the stiffness of the tube. Higher velocity corresponds to higher arterial stiffness.

It is generally agreed that many cardiovascular disorders are associated with increasing rigidity of the arterial wall.

II. Factors influencing arterial stiffness

A large number of publications and several reviews reported the various pathophysiological conditions associated with increased arterial stiffness (table 2). Apart from the dominant effect of ageing, they include physiological conditions, genetic background, CV risk factors, CV diseases and primarily non-CV diseases [3].

Table 2 Clinical conditions associated with increased arterial stiffness. Adapted from [3].

Ageing	CV risk factors	CV diseases
Physiological conditions	Hypertension	Coronary heart disease
Low birth weight	Smoking	Congestive heart failure
Menopausa Status	Obesity	Fatal stroke
Lack of physical activity	Hypercholesterolaemia	Primarily non-CV diseases
Genetic background	Impaired glucose intolerance	Moderate chronic kidney disease
Parental history of hypertension	Metabolic syndrome	Rheumatoid arthritis
Parental history of diabetes	Type 1 diabetes	Systemic vasculitis
Parental history of myocardial infarction	Type 2 diabetes	Systemic lupus erythematosus
Genetic polymorphisms	High C-reactive protein level	

When evaluating the degree of arterial stiffness, the two major parameters to be taken in account are age and blood pressure.

2.1.2 PWV Measurements

The measurement of PWV is generally accepted as the most simple, non-invasive, robust and reproducible method to determine arterial stiffness [3].

Carotid-femoral PWV is a direct measurement and it is the most clinically relevant, since the aorta and its first branches are the major components of arterial elasticity and they are responsible for most of the pathophysiological effects of arterial stiffness.

In addition, a large amount of epidemiological studies demonstrates that aortic PWV holds a strong predictive potential, as intermediate endpoint for CV events. In fact, it has a better predictive value than classical CV risks entering various type of risk score [1] [3-5].

PWV is usually measured using foot-to-foot velocity method from various waveforms. These are usually obtained at the right common carotid artery and right femoral artery, and the time delay (Δt or transit time) measured between the feet of the two waveforms (figure 1). A variety of different waveforms can be used including pressure, distension, and Doppler. For further reading: [2, 3].

The distance (D) covered by the waves is usually assimilated to the surface distance between the two recording sites.

PWV is calculated as:

$$PWV = \frac{D \text{ (meters)}}{\Delta t \text{ (seconds)}}$$

The distance should be measured precisely because small inaccuracies may influence the absolute value PWV. The shorter the distance between two recordings sites, the greater the absolute error in determining the transit time.

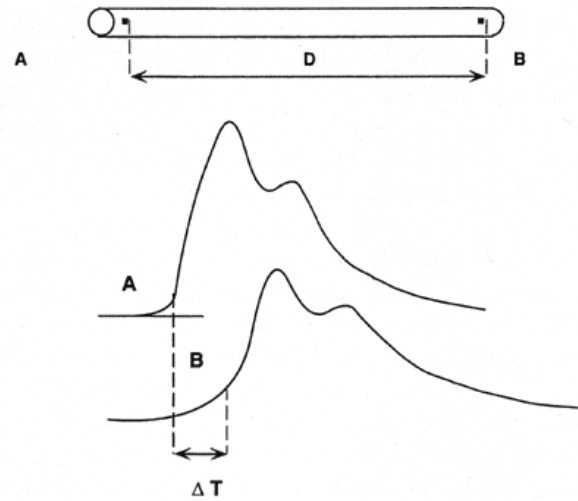


Figure 1 Measurement of PWV with the foot-to-foot method. Adapted from [4].

2.1.2.1 State of the art

The 'gold standard' for PWV's clinical evaluating are the Complior® (figure 2) and the Shpymocor® systems (figure 3), both based on pressure sensors. Since our goal is also the assessment of PWV it is useful to understand how these devices work.



Figure 3 The Complior® system [6].



Figure 2 The Sphymocor® system [7].

The Complior® system (Colson, France) employs dedicated mechanotransducers (PZ sensors - see Appendix A) directly applied on the skin. The transit time is determined by means of a correlation algorithm between each simultaneous recorded wave. The operator is able to visualize the shape of the recorded arterial waves and to validate them. Three main arterial sites

can be evaluated, mainly the aortic trunk (carotid-femoral) and the upper (carotid-brachial) and lower (femoral-dorsalis pedis) limbs [3] [6].

In the Shpymocor® system (ArtCor, Australia), a single high-fidelity applanation tonometer (Millar®) to obtain a proximal (i.e. carotid artery) and distal pulse (i.e. radial or femoral arteries) recorded sequentially a short time apart and calculates PWV from the transit time between the two arterial sites, determined in relation to the R-wave of the electrocardiogram¹ (ECG). The time between ECG and proximal pulse is subtracted from the time between ECG and distal pulse to obtain the pulse transit time. The initial part of the pressure waveform is use as a reference point. It is also possible to check offline the variability of measurement over a range of pulses, according to each algorithm [3] [7].

¹ See section 2.3.2.

2.2 Accelerometric Sensors

2.2.1 Introduction

Acceleration² is an important parameter for general-purpose absolute motion, orientation, tilt, vibration and shock sensing measurements and can be assessed by accelerometers [8].

Accelerometers are commercially available in a wide variety of ranges and types to meet diverse application requirements. Their **low-cost**, small size (MEMS³ devices), light weight and robustness, makes them a fundamental and increasingly common device in many technological areas.

In general, accelerometers are preferred over displacement and velocity sensors for the following reasons [9]:

1. They deliver 1, 2 or 3 measurement-axes and have a wide frequency range from DC to very high values, in such a way that steady accelerations can easily be measured;
2. Measurement of transients and shocks can be made more easily than with displacement or velocity sensing;
3. Displacement and velocity can be obtained by simple integration of acceleration (integration is preferred over differentiation).

In this section, common concepts underlying accelerometers usage (operation and calibration principles, main types and applications) will be briefly introduced.

2.2.2 General Concepts

Theory of operation

The accelerometer is described as a combination of two transducers: the primary one, a single degree of freedom vibrating mass or seismic mass, which converts the acceleration into a displacement (figure 4), and a secondary transducer which converts the displacement of the seismic mass into an electrical signal.

The spring-mass system, the basic physical principle behind most accelerometers design, is shown in the figure below.

² Acceleration is defined as the rate at which an object's *velocity* changes with time. Typical units: **m/s²** or '**g**'. 1g =9,81 m/s².

³ Micro Electro Mechanical Systems (MEMS) is the integration of mechanical elements, sensors, actuators, and electronics on a common silicon substrate through microfabrication technology [11].

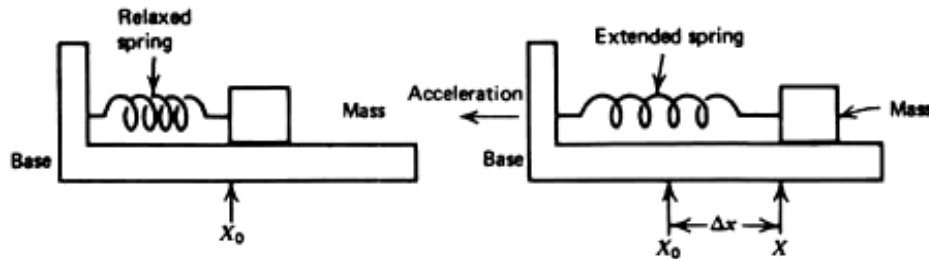


Figure 4 The basic spring mass system accelerometer [8].

A mass m that is free to slide on a base is connected to it by a spring. This spring that is in its unextended state exerts no force on the mass.

If this system undergoes a acceleration, then, by Newton's law, a resultant force equal to ma will be exerted on the mass. This force causes the mass to either compress or expand the spring under the constraint that $F=ma=kx$. Hence an acceleration a will cause the mass to be displaced by $x = ma/k$ or, conversely, if a displacement of x is observed, it is known that the mass has undergone an acceleration of $a = kx/m$.

Note that this model system only responds to accelerations along the length of the spring. This is referred to as a single axis accelerometer. In order to measure multiple axes of acceleration, this system needs to be replicated along each of the required axes.

Main types and applications

According to the type of secondary transducer accelerometers are generally classified as piezoelectric, potentiometric, reluctance, servo, strain gauge, capacitive or vibrating element. For further reading: [10].

Amongst its main application areas the following are worth mentioning:

1. Automotive (airbag sensors, active suspensions, roll over sensing, GPS, vibration monitoring, safety related testing)
2. Aeronautic and defence (ammunition & missile guidance, aeronautic instruments)
3. Medical (pacemaker, human motion analysis, wheel chair stabilization)
4. Industrial

Calibration

Calibration refers to the process of determining the relation between the output (or response) of a measuring sensor/instrument and the value of the input quantity, a measurement standard [9].

If the sensor has a linear response then its sensitivity⁴ is determined by the slope of the calibration curve.

An accelerometer can be calibrated by static or dynamic methods. To perform a static calibration of the accelerometer, the device is subjected to one or several levels of constant acceleration. The simplest method, for low g applications is to use the force of gravity, since it is the most stable, accurate and convenient acceleration reference available (figure 5) [12].

The dynamic calibration is usually obtained using an electrodynamic shaker. This device is designed to oscillate in a sinusoidal motion with variable frequencies and amplitudes.

The relationship between these variables, which are accurately measured, and the accelerometer's output is then determined.

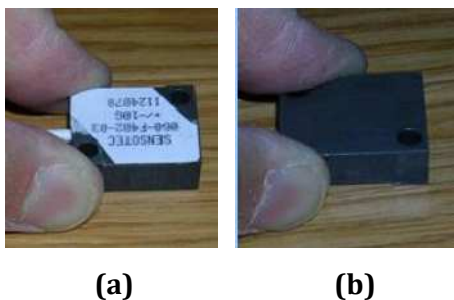


Figure 5 Flip Calibration [12]: **(a)** +1g **(b)** -1g.

To calibrate, the accelerometer's measurement axis is pointed directly at the earth. The 1 g reading is saved and the sensor is rotated 180° to measure -1 g . Using the two readings, the sensitivity is:

$$\text{Sensitivity} = [A - B]/2 g$$

A = Accelerometer output with axis oriented to +1 g ;

B = Accelerometer output with axis oriented to -1 g ;

⁴ The sensor's sensitivity measures the level of variation of the output regarding variations applied to its input. For example, an accelerometer is very sensible if small variations on the acceleration cause large variations in its output [9].

2.3 Electrocardiography

2.3.1 Introduction

One of the main techniques for diagnosing heart's electrical and mechanical condition is based on the electrocardiogram [13].

An electrocardiogram is a recording of the electrical activity on the body surface generated by the heart.

ECG measurement information is collected by skin electrodes placed at designated locations on the body. By convention, the electrodes are placed on each arm and leg, and six electrodes are placed at defined locations on the chest. The particular arrangement of two electrodes (one positive and one negative) with respect to a third one (the ground) is called a lead [14] [15].

There are three types of ECG leads: bipolar limb leads, augmented unipolar limb leads and unipolar precordial leads (table 3) [16].

In a standard clinical ECG, all leads are recorded simultaneously, giving rise to what is called a 12-lead ECG. In monitoring applications, typically one or two leads are used, since the principal goal of these is to reliably recognize each heartbeat and perform rhythm analysis [13].

Table 3 Types of ECG leads. The bipolar leads utilize a single positive and a single negative electrode between which electrical potentials are measured. The unipolar leads have a single positive recording electrode and utilize a combination of the other electrodes to serve as a composite negative electrode. Each of the 12 leads provides spatial information about heart's electrical activity in three approximately orthogonal directions: right \leftrightarrow left; superior \leftrightarrow inferior; anterior \leftrightarrow posterior [5] [6]. Lead place diagrams can be seen in Appendix A.

Leads Types		Electrodes Location	Electrical activity recorded: Spatial Information	
Bipolar Limb	I	RA (-) to LA (+) ¹	Frontal Plane	Right Left, or lateral
	II	RA (-) to LF (+)		Superior Inferior
	III	LA (-) to LF (+)		Superior Inferior
Unipolar	Augmented	aVR		Rightward
		aVL		Leftward
		aVF		Inferior
Precordial	Chest	V ₁ , V ₂ , V ₃	Horizontal Plane	Posterior Anterior
		V ₄ , V ₅ , V ₆		Right Left, or lateral

¹ RA: right arm; LA: left arm; LF: left foot

(-) negative electrode, (+) positive electrode

2.3.2 Components of the ECG

The ECG signal is characterized by six peaks and valleys labelled with successive letters of the alphabet P, Q, R, S, T and U [14]. Figure 6 shows a typical ECG tracing of a normal cardiac cycle, which consists of a **P** wave, a **QRS** complex, a **T** wave and a **U** wave⁵. The presence and polarity of these components depend on the position of the electrodes on the body.

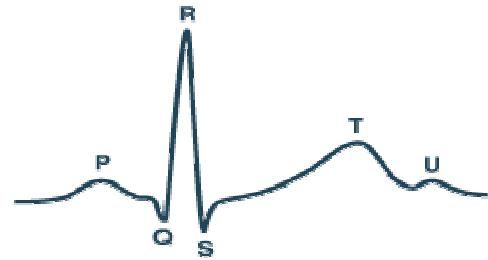


Figure 6 Form of a normal ECG signal

[14]

Cardiac Cycle (CC) ⁶

The CC is the sequence of events that occur in the heart from the beginning of one heart beat to the beginning of the next.

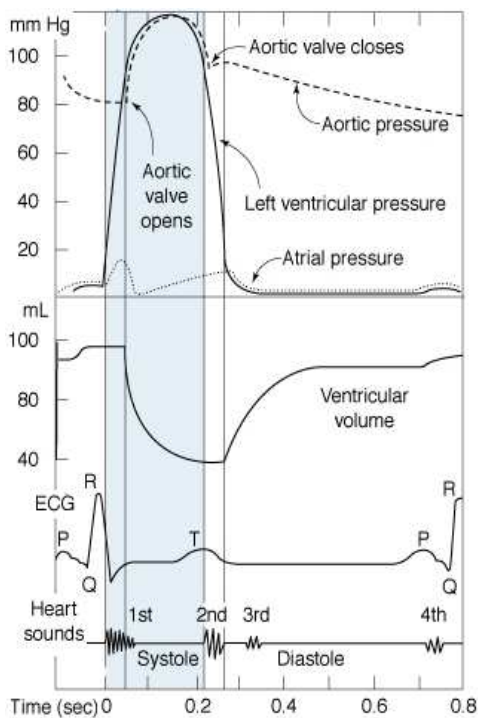


Figure 7 Cardiac Cycle Diagram.

Changes in aortic pressure, left ventricular pressure, left atrial pressure, left ventricular volume and heart sounds during a single CC, are related in time to the ECG. Adapted from [20].

The diagram shown to the left (figure 7) depicts the relationship between the ECG and the mechanical (pressure, volume) and valvular events occurring in one CC.

A single cycle of cardiac activity can be divided into two basic stages: **diastole**, which represents ventricular filling and a brief period just prior to filling at which time the ventricles are relaxing; and **systole**, which corresponds to the time of contraction and ejection of blood from the ventricles into aorta and pulmonary artery [19].

In an ECG, the beginning of systole is marked by the appearance of the QRS complex. In contrast, the diastole period is bounded by the end of T wave and the beginning of the next P wave.

To analyze these two stages in more detail, the CC is usually divided into seven phases: Atrial Contraction, Isovolumetric Contraction, Rapid Ejection, Reduced Ejection, Isovolumetric Relaxation, Rapid Filling and Reduced Filling. For further reading on this issue: [19].

⁵ The normal values associated to ECG components can be seen in the Appendix A.

⁶ In order to understand this issue, it is possible to review basic cardiac anatomy also in the Appendix A.

Regulation of Cardiac Cycle

The rhythmic contractions of the heart occur in response to periodic electrical impulse sequences. It is the conduction of an electrical impulse from the top of the heart over the atria through the septum and the ventricles that causes the cardiac muscle contraction, the opening and closing of the valves and the blood flow into the body (figure 8a).

The sinoatrial node (SA node) or heart's pacemaker is the generator of the electrical signal, initiating each CC. When SA node depolarizes the electrical stimulus spreads through atrial muscle, which leads to the contraction of both atria - this event can be seen in ECG as P wave - then the electrical impulse flows down to the lower chambers of the heart, stimulating the ventricles to contract (QRS Complex). Finally, the electrical

current spreads back over the ventricles in the opposite direction. This activity is called the recovery wave, which is represented by the T wave [15] [16]. Sometimes, after T wave it may be seen the U wave. The origin of this is still in question, however most of the researchers correlate it with the repolarization of a collection of specialized muscle fibers in the ventricles (Purkinje fibers) [23].

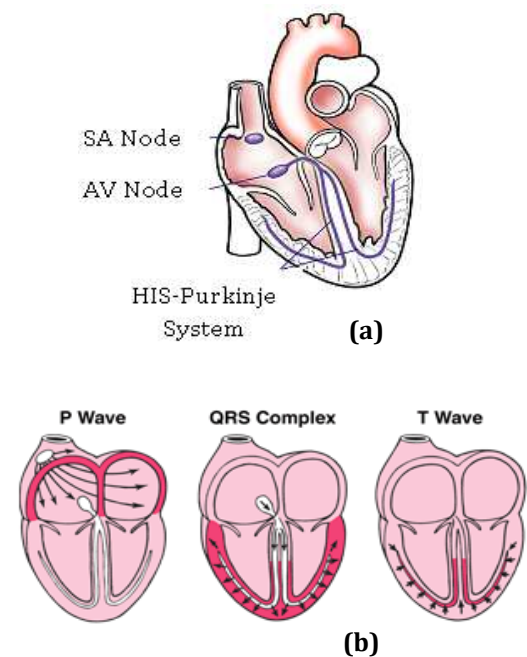


Figure 8 Heart's electrical activity (a) Conduction system (b) Electrical Sequence. Adapted from [21] [22]

2.3.3 Instrumentation Requirements

Signal Acquisition Challenges

The front end of an electrocardiograph must be able to deal with extremely weak AC signals ranging from 0.5mV to 5.0 mV, combined with a DC component of up to ± 300 mV - resulting from the electrode-skin contact -plus a common mode component of up to 1.5 V, resulting from the potential between the electrodes and ground [14]. The useful bandwidth of an ECG signal, depending on the application, can range from 0.05 Hz to 50 Hz- for a monitoring application in intensive care units - up to 1 kHz for late potential measurements (pacemaker detection). A standard clinical ECG application has a bandwidth of 0.05 Hz to 100 Hz.

ECG signals may be corrupted by various kinds of noise, such as [14]:

- Power-line interference: 50–60 Hz pickup and harmonics from the power mains;
- Electrode contact noise: variable contact between the electrode and the skin, causing baseline drift;
- Motion artefacts: shifts in the baseline caused by changes in the electrode-skin impedance;
- Muscle contraction: electromyogram-type signals are generated and mixed with the ECG signals;
- Respiration, causing drift in the baseline;
- Electromagnetic interference from other electronic devices, with the electrode wires serving as antennas;
- Noise coupled from other electronic devices, usually at high frequencies;

For meaningful and accurate detection, it is necessary to filter out all these noises sources.

Typical Measurement System

Figure 9 shows a block diagram of a typical single-channel electrocardiograph. The ECG system comprises five basic stages. In the first one the bioelectrodes convert the ionic current flow of the body to an electron flow of the metallic wire. The efficient acquisition by these electrodes relies on a gel with a high ionic concentration. This acts as the transducer at the tissue-electrode interface ^[16].

Then an instrumentation amplifier (IA), with a high gain and common mode rejection ratio (CMRR), attenuates the signals that are common to both inputs and amplifies the difference between the two signals. Due to this some of the noise is eliminated. To further reject 50Hz and 60 Hz noise, an operational amplifier (op amp) deriving common-mode voltage is used to invert the common-mode signal and drive it back into the patient trough the right leg ^{[14][24]}.

Subsequently, it is visible the presence of an opto isolator⁷, which allows galvanic isolation; some analog filters (high pass filter, low pass filter and notch); an ADC⁸ and a DSP⁹, which permit the conversion to digital domain and the communication to computer, respectively^[14].

⁷ This technology can be substituted by other with the same function, e.g.: magnetic induction.

⁸ Analogic Digital Converter.

⁹ Microprocessor or Microcontroller.

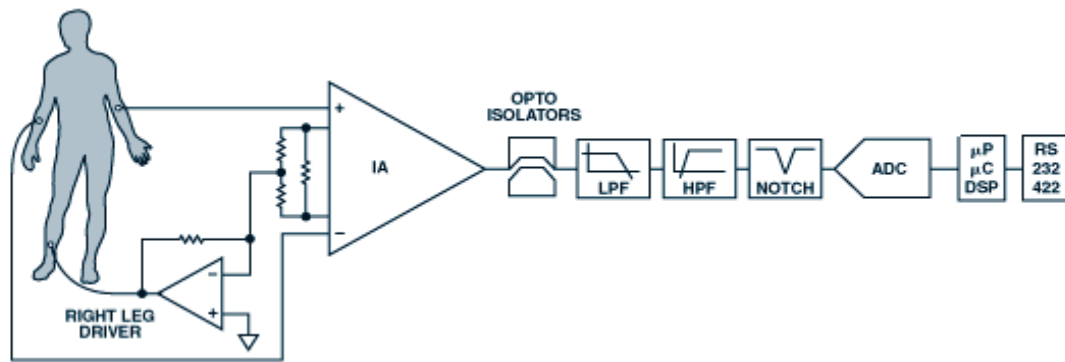


Figure 9 Typical single-channel electrocardiograph. Adapted from [14].

References

- [1] Nichols, W.W. and O'Rourke, M.F., *McDonald's Blood Flow in Arteries: Theoretical, Experimental and Clinical Principles*, 5th ed. London: Hodder Arnold, 2005, pp. 54-72
- [2] Xu, Minnan., "Local Measurement of the Pulse Wave Velocity using Doppler Ultrasound." Master's Thesis, Massachusetts Institute of Technology, 2002
- [3] Laurent, S. et al, "Expert consensus document on arterial stiffness: methodological issues and clinical applications", Special article, *European Heart Journal*, 27, pp. 2588-2605, Sep.2006
- [4] Safar, M. et al, "Aortic Pulse Wave Velocity: an Independent Marker of Cardiovascular Risk", *J Geriatr Cardiol*, 11, pp.295-298, 2002
- [5] Blacher, J. et al, "Aortic Pulse Wave Velocity as a Marker of Cardiovascular Risk in Hypertensive Patients", *Hypertension*, 33, pp.1111-1117, 1999
- [6] Figure at: <http://www.pmsinstruments.co.uk/Complior%20SP.htm>
- [7] Figure at: <http://atcormedical.com/sphygmocor.html>
- [8] Pereira, Helena, "Acelerómetros". Monography, *Sensores e Sinais Biomédicos* discipline Universidade de Coimbra, January 2006
- [9] Webster, John G., *Measurement, Instrumentation and Sensors Handbook CRCnetBASE*. 1st ed. New York: CRC Press LLC, 1999, pp: 454-481
- [10] Muramatsu, Brandon. "Accelerometer." 16 Jan 2000. University of Berkeley. 7 Sep 2007 http://bits.me.berkeley.edu/beam/acc_1.html
- [11] "What is MEMS Technology?." *MEMS and Nanotechnology Clearinghouse*. MEMS and Nanotechnology Clearinghouse. 7 Sep 2007 <http://www.memsnet.org/mems/what-is.html>
- [12] Stilson, Tim. "Accelerometer." *Input/Data Acquisition System Design for Human Computer Interfacing*. 17 Oct 1996. 7 Sep 2007 <http://soundlab.cs.princeton.edu/learning/tutorials/sensors/node9.html>
- [13] Tompkins, J. Willis, *Biomedical Digital Signal Processing*, Prentice-Hall, Inc., 1993, pp.24-39
- [14] Bosch, E., "ECG Front-End Design is Simplified with MicroConverter", *Analog Dialogue* 37-11, November 2003, www.analog.com/analogdialogue

- [15] Biopac Systems, Inc., "Lesson 5 Electrocardiography I", Physiology Lessons for use with the Biopac Student Lab, www.biopac.com
- [16] Berbari, E.J., "Principles of Electrocardiography", *The Biomedical Engineering Handbook*, 2nd ed. Boca Raton: CRC Press LLC, 2000, Chapter 13
- [17] Yanowitz, Frank. "Lesson 1: The Standard 12 Lead ECG." *ECG learning center*. 5 Jun 2006. 2 Sep 2007 http://library.med.utah.edu/kw/ecg/ecg_outline/Lesson1/index.html
- [18] Klabunde, Richard . "ECG leads." *Cardiovascular Physiology Concepts*. 01 Jan 2007. 2 Sep 2007 <http://cvphysiology.com/Arrhythmias/A013.htm>
- [19] Klabunde, Richard . "ECG leads." *Cardiovascular Physiology Concepts*. 13 Apr 2007. 2 Sep 2007 <http://cvphysiology.com/Heart%20Disease/HD002.htm>
- [20] Figure at: http://connection.lww.com/Products/porth7e/documents/Ch23/jpg/23_015.jpg
- [21] Figure at: <http://www.heartcare4u.com/hearts/normalheart.jpg>
- [22] Figure at: www.merck.com/mmhe/sec03/ch021/ch021c.html
- [23] Yanowitz, Frank. "Lesson 12: Nice Seeing U wave." *ECG learning center*. 5 Jun 2006. 2 Sep 2007 < http://library.med.utah.edu/kw/ecg/ecg_outline/Lesson12/index.html >
- [24] TI medical applications
- [25] Figure at: http://www.bg.ic.ac.uk/Staff/khparker/homepage/BSc_lectures/2002/Heart_anatomy.jpg
- [26] Figure at: <http://www.doc.ic.ac.uk/~giso/projects/arrhythmia/node4.html>
- [27] Figure at: www.publicsafety.net/12lead_dx.htm
- [28] Figure at: www.cvphysiology.com/Arrhythmias/A013c.htm
- [29] Figure at: <http://butler.cc.tut.fi/~malmivuo/bem/bembook/15/15.htm>

CHAPTER 3

PROCESS METHODOLOGY

This chapter presents the work developed by the hemodynamic team, previously to the Project starting date, in the field of cardioaccelerometry.

3.1 Introduction

The development of an accelerometer based instrument started some months before the beginning of the Project discipline. At that time, its application was related with the maintenance and monitoring of railways equipments.

However, lab experiments were carried out using the same instrument in the carotid artery of human subjects, showing promising results.

The potential of these results was then discussed with a cardiologist and a new objective arose: the assessment of PWV with accelerometers. In order to achieve this idea a first accelerometer based instrument was designed and trimmed to clinical experiments.

3.2 Measurement System Architecture

The first measurement system developed for *in situ* clinical research tests (CTs) is shown in figure 10. It can be divided into three different blocks: the accelerometer based probe and the data acquisition (DAQ) module, that constitute the instrument itself, and the data processing block.

The measurement probe consists of a cylindrical piston (diameter: 5,1mm; length: 14,7mm) rigidly coupled to the electronic circuit, which is protected by a plastic box (78,8mm×39,0mm×22,0mm).

The acceleration transmitted to the piston is measured by the in-circuit dual-axis accelerometer ADXL203CE¹⁰, featuring a full-scale range of ±1.7g. The voltage signal generated by this is then filtered, in order to cancel the DC component associated to gravity, and amplified (see circuit at Appendix B). The preference towards this accelerometer resulted from some estimates.

¹⁰ Data sheet: http://www.analog.com/UploadedFiles/Data_Sheets/ADXL103_203.pdf.

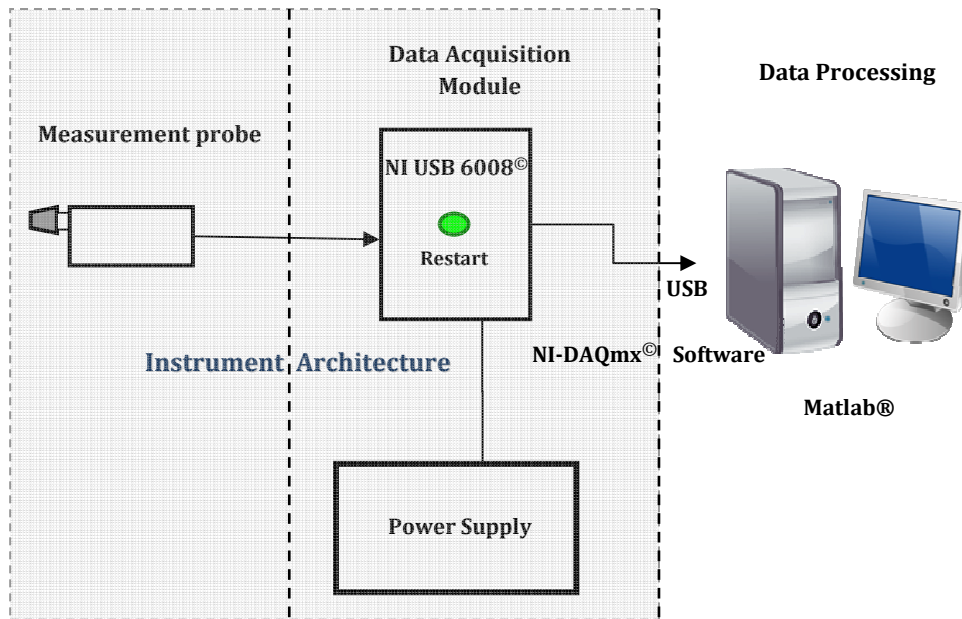


Figure 10 General measurement system architecture.

The DAQ module used in this measurement system is the NI USB-6008^{®11}, shown in figure 11. This device is based in an 8051 microcontroller, can sample up to 10Ks/s and comes with a driver software for interactive configuration and data acquisition running on Windows Operative System: the NI-DAQmx[®] (table 4). This software includes VI Logger Lite, a configuration software package, which is used in this architecture for data logging.

After the data logging, it follows up the data processing, where the files are saved in a .txt format and processed in Matlab[®].

Table 4 Some NI USB-6008 Specifications^[1].

Specifications Summary

USB Bus Type
8 analog inputs (resolution: 12-bit; sampling rate: 10Ks/s);
2 analog outputs (resolution: 12-bits; update rate: 150Ks/s);
12 digital input/output;
32-bit counter;
NI-DAQmx [®] driver software and NI LabVIEW SignalExpress LE interactive data-logging software;



Figure 11 NI USB-6008[®] [1].

¹¹ Data sheet at: <http://www.ni.com/pdf/products/us/20043762301101dlr.pdf>.

3.3 Clinical Trials

3.3.1 Data Acquisition

In order to acquire data, the instrument shown in figure 12 was taken to IIFC, where for a one month time period tests in 21 young and healthy subjects were carried out.

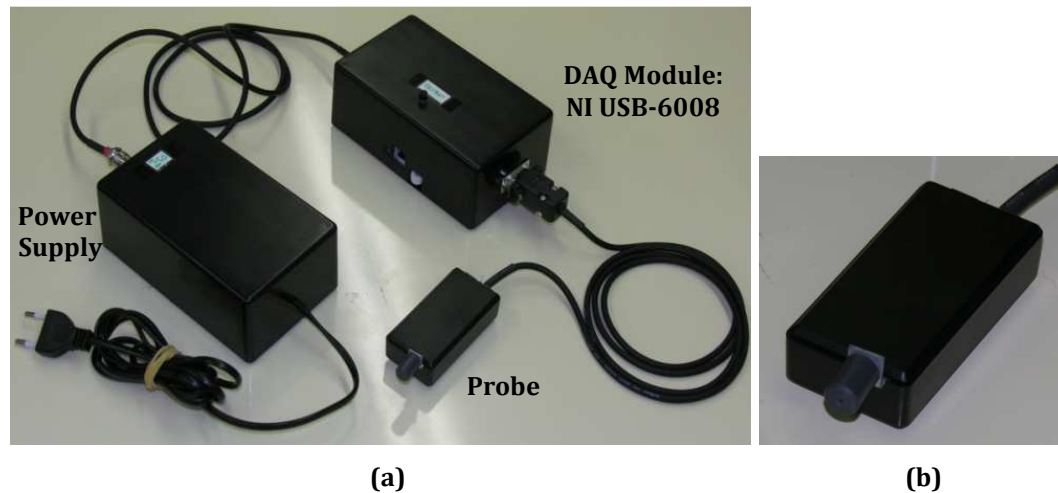


Figure 12 Developed Instrument.

(a) General device: The power supply must be connected to DC Power Supply and the DAQ Module to PC (with VI Logger) by an USB cable. **(b)** Zoomed measurement probe.

The procedure consisted on the following steps: after switching on the instrument and starting the VI Logger application, the patient was laid down. Then, the measurement probe was placed on the carotid or femoral arteries, and its position slightly adjusted until a relevant signal started to be seen. From that moment on, and during 10-20 seconds, data was acquired. The logged data was finally saved in a .txt file with an appropriate tag name.

3.3.2 Data Processing¹²

Once the data have been collected, it was necessary to proceed to their analysis in order to draw conclusions.

The clinical data processing was made in Matlab®, and started by their general visualization. The recognition of a specific pattern for carotid and a different one for femoral data was immediately recognized. The characteristic pattern consists of two successive peaks for the carotid and just one for the femoral (figure 13).

¹² The clinical data processing marked the official beginning of the Project discipline.

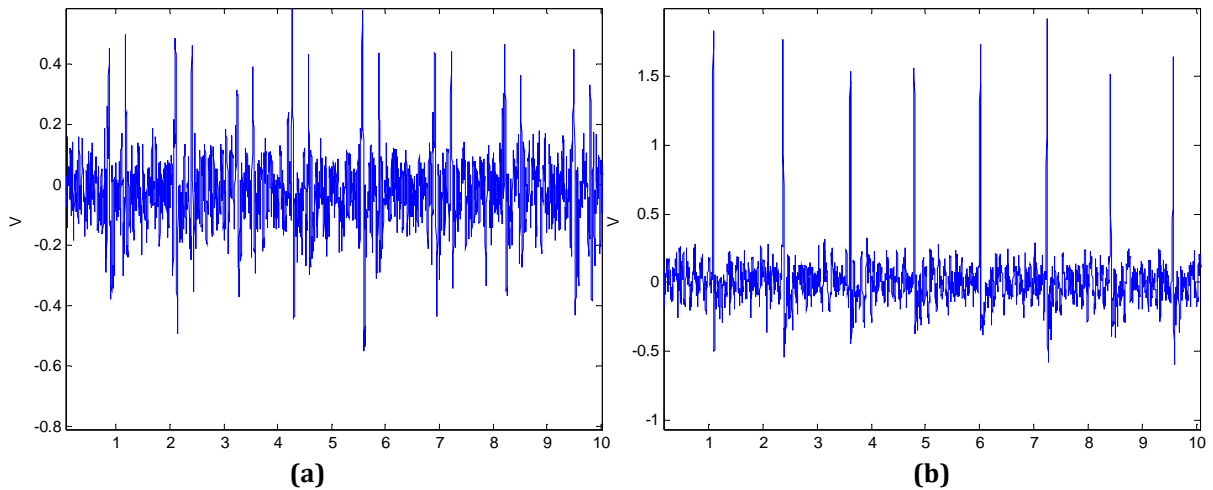


Figure 13 Original Signals of a young and healthy subject, obtained with the accelerometer based instrument and visualized in Matlab®: (a) Carotid signal. (b) Femoral Signal.

In order to extract more information about patterns repeatability, an algorithm was developed, whose main purpose was to relate the peaks of each acquisition.

This algorithm consisted in the following main steps:

Step 1: File loading and visualization;

Step 2: Filtering (application of a band-pass filter);

Step 3: Selection of peaks;

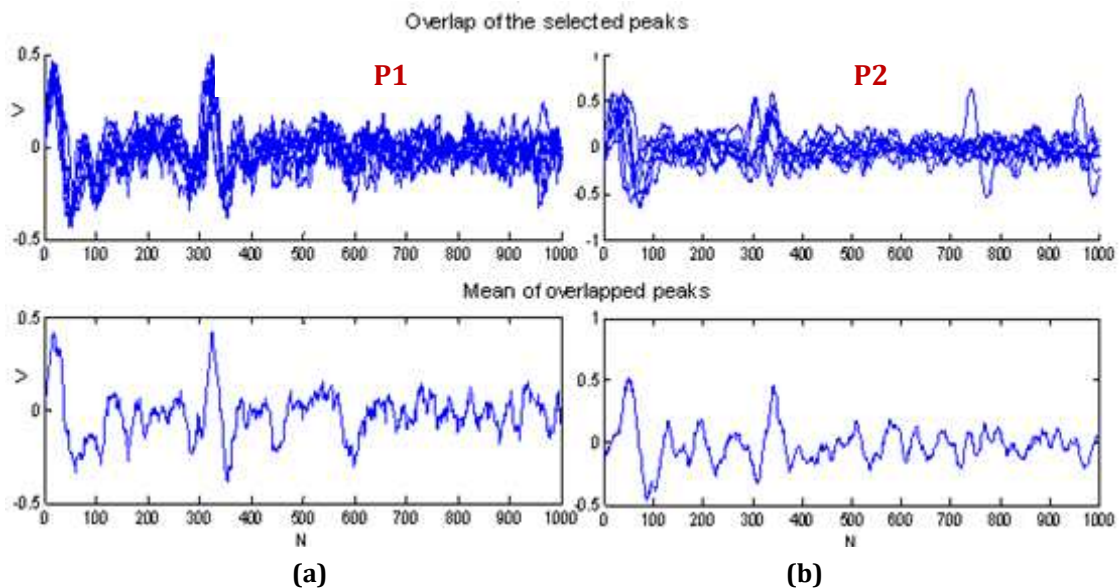
Step 4: Peaks Adjustment;

Step 6: Overlapping of the selected peaks;

Step 7: Mean determination of overlapped peaks;

Step 8: Data saving.

Figure 14 shows the result from the application of steps 6 and 7 to either a carotid or femoral files of two patients.



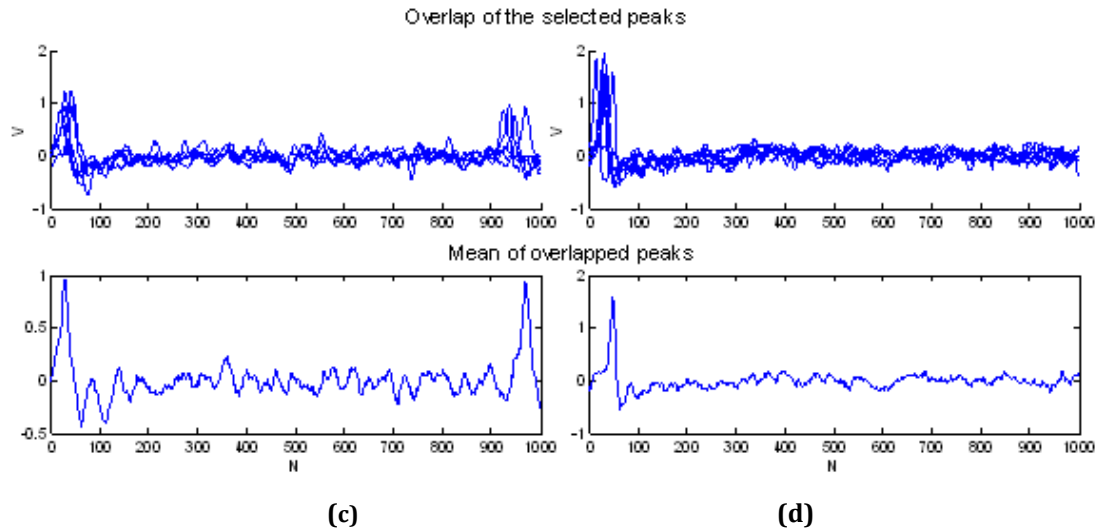


Figure 14 Overlap of eight selected peaks and mean of these overlapped peaks.
(a) Carotid data of patient 1. **(b)** Carotid data of patient 2. **(c)** Femoral data of patient 1.
(d) Femoral data of patient 2.

After this analysis method was applied to all the data, the pattern described previously was confirmed: two peaks for carotid files and one peak for femoral files. Besides, only two more common aspects were seen: the first one was that the majority of files presented high levels of noise, even after filtering. The second one was that each patient had a unique and singular signal, distinguishable from the others.

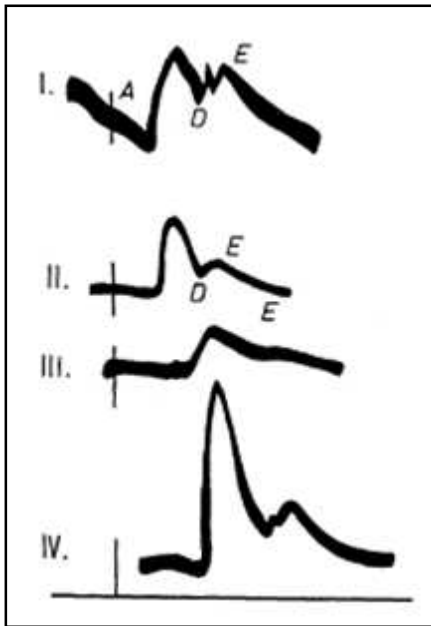
3.4 Discussion

The performed data processing was only a first approach to understand the type of information that could be extracted from the accelerometer based instrument and, at this point it cannot be conclusive. In fact, it was only a basic method to determine the aspects that could be improved. The first aspect relates to the high levels of noise in the signals which must be avoided, and the second one is related with the need of including another type of signal which could serve as a reference.

In order to solve these problems, we concluded that it would be necessary to improve the instrument electronics and to integrate ECG or PZ based signals, turning it into a multisensor prototype.

Regarding the pattern seen in the acquired data, we concluded that there was a good agreement between this and the pulse wave contour in carotid and femoral arteries. As it is shown in figure 15, the pulse wave in carotid artery shows the *incisura dicrota*¹³ and the dicrotic

¹³ The high frequency wavelet on an arterial pressure wave due to sudden closure of the aortic or pulmonary valve.



wave ¹⁴ in contrast with the femoral artery which does not show any of them. This fact suggested that the second peak seen at the data collected in carotid artery matched the dicrotic wave only seen in the upper arteries.

Figure 15 Pulse wave Contour in some arteries.

I. Carotid; II. Brachial; III. Radial; IV. Femoral.
 A. Auricular systole; D- Incisura Dicrota; E- Dicrotic wave.
 Adapted from [2].

References

- [1] Figure and specifications at: <http://www.ni.com/pdf/products/us/20043762301101dlr.pdf>.
 [2] "Pulso Arterial." Biblioteca Digital de la Universidad de Chile. 2 Sep 2007 http://mazinger.sisib.uchile.cl/repositorio/lb/ciencias_quimicas_y_farmaceuticas/steinera/part_e04/02d.html

¹⁴ A diastolic wave following the systolic peak. This is the echo of the first wave following its reflection in the peripheral vasculature.

CHAPTER 4

MEASUREMENT PROBES

The design of the measurement probe is crucial to the success of an efficient accelerometric instrument. This is the reason why this chapter is entirely devoted to the description of the several versions developed throughout this project.

Note – Some concepts depicted in this chapter may be protected by international patents.

4.1 Introduction

The analysis of the first data bunch (section 3.3.2) immediately showed a number of drawbacks and, consequently, the need to improve the instrument in many ways.

Concerning the measurement probe, the first perception was that the mechanical coupling between the pulsating tissues and the sensor was not efficient which greatly impaired the signal to noise ratio at the output.

It was very clearly the need to modify the rigid coupling between the piston and the electronic circuit, identified as a major noise source. In fact, the second version of the measurement probe arose from this adjustment and it featured a spring loaded coupling between the piston and the sensor. It was therefore designated as **spring-loaded probe (SLP)**.

Clinical experiments carried out with the SLP (chapter 8), however, showed that the final noise level, mainly the one that was attributed to the operator itself, was still very high. A new design was sorted out to remove this problem and another was built, based on a mechanically differential scheme that used two aligned accelerometer sensors. For obvious reasons, we have named this probe **differential probe (DP)**.

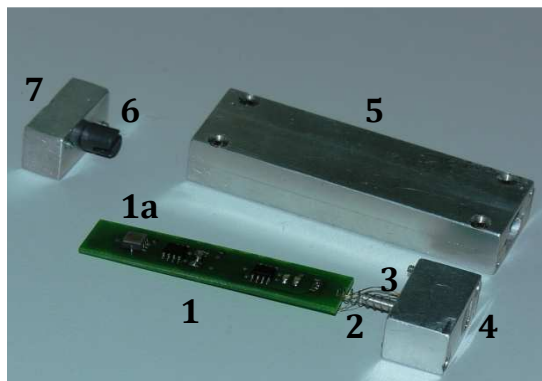
The fourth and last probe version was developed in the final stage of this work and joined the concepts of all the other versions adding the ability of integrating a PZ transducer into the piston. This **probe**, which we called **hybrid**, was used only for data acquisition in the pulsatory model, described in chapter 7.

4.2 Spring-Loaded Probe

The configuration of the SLP, the second measurement probe, is shown in figure 16.

As mentioned, in this version the coupling is based on a spring-loaded mechanism. The used high quality spring ($k= 0,06 \text{ N/mm}^{15}$; $\varnothing_{\text{ext}}=3,45\text{mm}$; $l=10\text{mm}$) at rest is held in position by a 2 mm wide guiding post¹⁶ and is connected to the electronic circuit at its rear side, through two small filed cuts.

The front side of the circuit is fitted to a cylindrical shaped piece of PVC¹⁷, which is, in turn, attached to the cylindrical piston¹⁸ ($r=5,0 \text{ mm}$) through an appropriate mechanical rigid link.



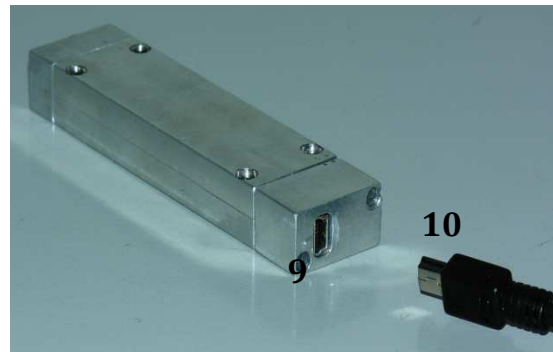
(a)

The probe's covering ($104,3\text{mm} \times 24,8\text{mm} \times 13,1\text{mm}$) consists of three metal pieces: the main body, where the electronic circuit slides, and the frontal and rear blocks, where the piston and a mini-USB are incorporated, respectively.

The mini-USB receives the accelerometer signal and provides power to the circuit through extremely thin ($90\mu\text{m}$) enameled



(b)



(c)

Figure 16 SLP. (a) Exploded view; (b) Assembled front side; (c) Assembled rear side; 1- Electronic circuit; 1a) Accelerometer; 2-Spring with guiding post; 3- Connecting copper wires; 4- Back covering block; 5-Main covering body; 6-PVC support piece; 7- Front covering block; 8- Cylindrical Piston; 9-Mini-USB; 10- Mini-USB cable;

copper wires.

The signal is then connected to the acquisition module by an USB cable.

¹⁵ It is a very small spring constant.

¹⁶ The guiding post is an integral part of the rear covering block.

¹⁷ Polyvinyl Chloride.

¹⁸ It is also made of PVC plastic.

The presented electronic circuit also contains the ADXL203CE accelerometer with capacitive coupling and a gain stage (≈ 20). The circuit schematic can be seen at Appendix B.

Model of the Spring-Loaded Mechanism

A close examination of the SLP's mode of operation shows that it is possible to establish a relationship between the force exerted on the piston (F), the spring displacement (x), the probe's movable mass (m), and the acceleration of the movable mass (a), through the Newton's second law:

$$F - kx = ma \quad (\text{Eq. 2})$$

where, k = spring constant in N/m

$$[F] = \text{N};$$

$$[x] = \text{m};$$

$$[m] = \text{Kg};$$

$$[a] = \text{m/s}^2$$

The forces which act on the movable assembly¹⁹ are: the force due to the pulse wave propagation, which can be given by $F=PS$ (P =pressure associated to pulse wave propagation; S =section of the piston)

and, the force due to spring's compression, F_1 , given by $F_1=k.x$ (figure 17).

In a first approach, it is possible to estimate the pressure value associated to pulse wave propagation, in a given location, by:

$$P = \frac{ma + A}{S} \quad (\text{Eq. 3})$$

Since the displacement of the loaded spring is very small, the term $k.x$ is considered constant (A).

4.3 Differential Probe

The construction of the DP was motivated by the analysis of data acquired at IIFC using the SLP and, it arose mainly from the need of avoiding the artefacts introduced by the operator itself.

¹⁹ Piston+ support piece+ electronic circuit +spring.

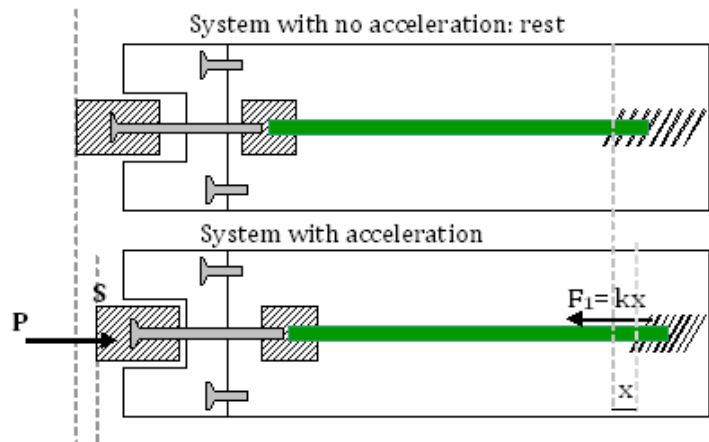


Figure 17 Schematic of the forces applied on the SLP during data acquisition.

Figure 18 pictures the DP's external aspect. The covering ($102,3\text{mm} \times 24,8\text{mm} \times 12,7\text{mm}$) is also made of metal (aluminium) and comprises the main body and the two extremities. The front extremity is rounded off in order to make the DP more ergonomic and, the PVC cylindrical piston ($r=5,0\text{mm}$) is less prominent than the SLP's piston.

The DP also features a spring-loaded mechanism. In fact, the only difference from the SLP's mechanism is that the spring ($k= 0,06 \text{ N/mm}$; $\varnothing_{\text{ext}}=3,45\text{mm}$; $l=12,1\text{mm}$) is set with a different compression force²⁰.

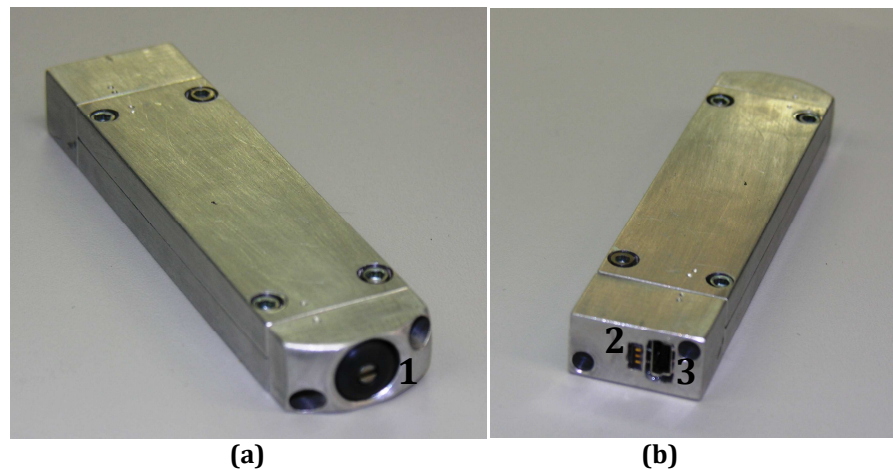


Figure 18 DP. (a) Assembled front side. (b) Assembled rear side.
1- Movable Piston; 2- Fixed accelerometer; 3- Mini-USB

The main innovation for the DP resides on its **mechanically differential structure**, which is achieved by the action of an extra accelerometer (ADXL203CE) that is fixed to the bulk of the probe. Assuming that both accelerometers are equally oriented and well aligned, the output signals of both can be electronically subtracted in order to remove all common acceleration components in such a way that only the pulsatile acceleration, from the piston-attached accelerometer, remains to be analogued.

The electronic circuit²¹ is based on the INA126²² IA and on the TL082 inverting op amp. The INA126 (Gain ≥ 5) is an important component on this circuit, since it amplifies the difference between the signals of the fixed and the floating accelerometers and nulls the signals that are common to both inputs.

²⁰ Compression (Δx) = $0,8\text{mm} \leftrightarrow$ Force exerted by the spring $=k \cdot \Delta x=0,006 \times 0,8=48\text{mN}$.

²¹ The printed circuit board (PCB) used for the DP's electronic circuit was the same of the SLP. Since the electronic circuits of the two probes were different, it was necessary to remove and add some connections of the DP's PCB.

²² Data sheet at: <http://focus.ti.com/lit/ds/symlink/ina126.pdf>.

As mentioned, the fixed and the floating accelerometers must be perfectly aligned and with the same orientation, in order to guarantee the mechanically differential scheme. In this way, the difference between their outputs will be zero when they have the same movement or the probe is at rest.

4.4 Hybrid Probe (HP)

The HP was the last version of the measurement probes to be developed. Although it has not been tested in the clinical environment, it was tested in the pulsatory model (chapter 7).

This probe is an improved version of the DP, since it combines the spring-loaded and differential mechanisms with an important source of information: a PZ transducer on the top of the piston.

The placing of the PZ transducer on the piston implied some slightly changes in the configuration of the probe, as is shown in figure 19.

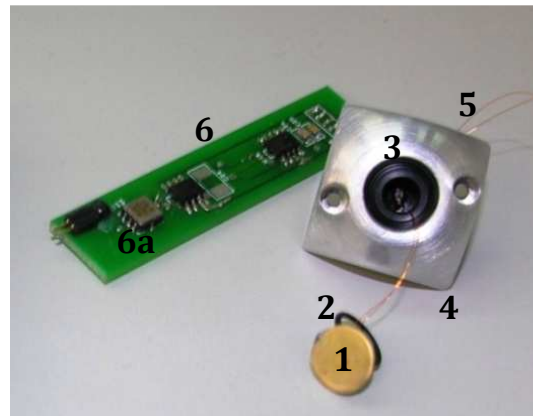
The anterior extremity (25mm×25mm×12,8mm) of the metal covering²³ is squared, with rounded edges and presents an “o”ring that is attached to the PZ transducer, in order to improve the adjustment of the tip to the acquisition location. The PZ signal is connected to the electronic circuit by two enameled copper wires (signal and ground), that go through the piston and the support piece.

The electronic circuit consists basically of the ADXL203 accelerometer, and the IAs, INA126 and INA121. The INA126, is set for a gain of 5 and, as in the DP, it amplifies the difference between the accelerometer outputs. The INA121²⁴, with unitary gain, suppresses the noise pickup produced by the PZ transducer. Besides that, it presents current feedback via two resistors of 8.2M, in order to eliminate guarding and achieve insulation requirements [1].

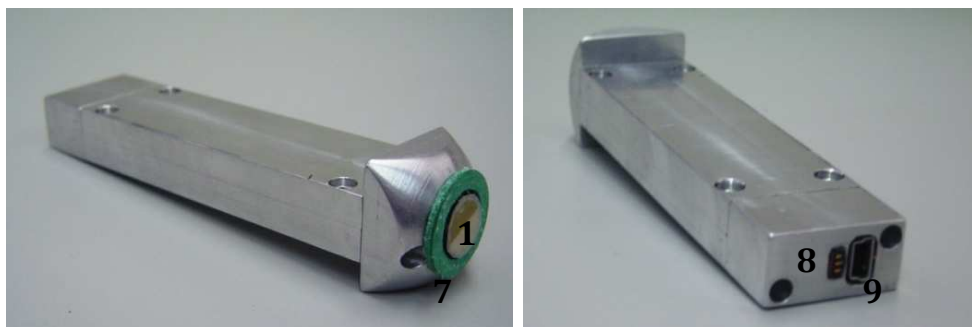
Appendix B shows a schematic that will allow a fully detailed understanding of the circuit.

²³ Probes covering: 105,9mm×25mm×12,8mm.

²⁴ Data sheet at: <http://focus.ti.com/lit/ds/symlink/ina121.pdf>.



(a)



(b)

(c)

Figure 19 Hybrid Probe. (a) Electronic circuit and front side block; **(b)** Assembled lateral side; **(c)** Assembled rear side; 1- PZ Transducer; 2- "O"ring; 3- Movable piston; 4- Front covering; 5- Copper wires; 6- Electronic circuit: **a)** Floating accelerometer; 7- Support ring of the piston; 8- Fixed accelerometer; 9- Mini-USB.

References

- [1] Wuchinich, Dave. "Circuit suppresses capacitively coupled noise pickup by the piezoelectric sensor and its wiring." *EDN: Design ideas* 23 11 2006 75-76. 15 Aug <http://www.edn.com/article/CA6391432.html>

CHAPTER 5

DAQ MODULES

As the measurement probes were being developed, it was also necessary to adjust the DAQ module to their requirements.

Since five versions of the DAQ module were constructed to achieve this purpose, this chapter depicts their principal features and successive improvements.

5.1 Introduction

The instrument enhancement involved not only the probe's design upgrade but also the development of a multichannel platform, which could integrate different hemodynamic signals.

In fact, the addition of different sensor types to the DAQ module came out from the need of having several time references to allow accelerometric signal comprehension.

The first DAQ module version could only accommodate the SLP and the ECG sensors, in opposite to the last one (fifth version) which already included the HP, the electrocardiograph, two PZ transducers and one pressure sensor and an independent $\pm 5V$ DC power supply.

Whether regarding the number of information channels or the signal to noise ratio (SNR) at the output, each new version was actually better than the previous one.

5.2 Module A

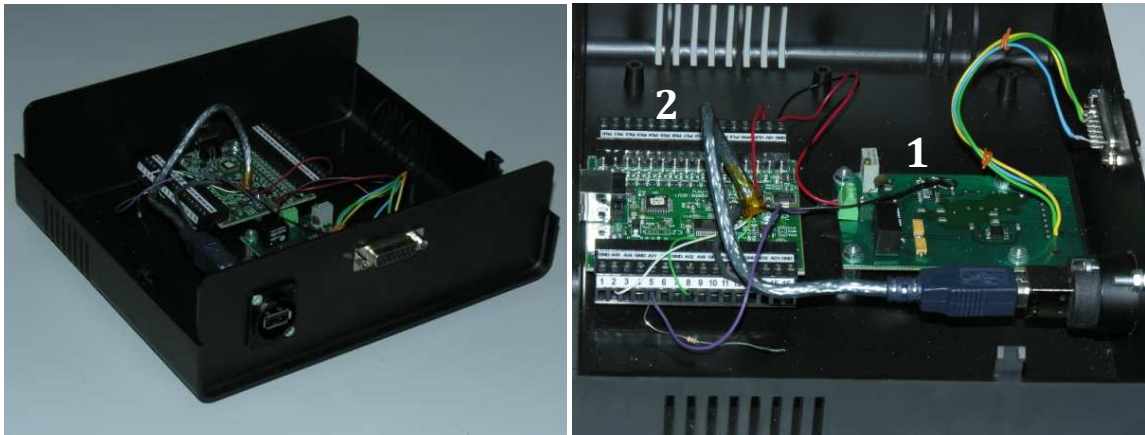
As it is shown in figure 20, the first developed DAQ module comprised only an electrocardiograph (to provide a starting time reference) and the NI USB-6008©.

The electrocardiograph circuit is based on the single-channel scheme described in section 2.5.3 and consequently it presents four electrodes which are placed on the body in agreement with the configuration of lead I.

The analogue front-end (see circuit schematic at Appendix B) applies the typical approach with an IA and a right leg common-mode feedback op amp. An AD620²⁵ set to a gain of 9 is used as IA and, a TL081 op amp is used to cancel the common mode interference. A variable gain block follows, which allows for the adjustment of the output voltage signal, and a protection

²⁵Data sheet at: http://www.analog.com/UploadedFiles/Data_Sheets/37793330023930AD620_e.pdf.

block with back-biased diodes is placed on the signal path in order to provide protection from over voltages. Power is supplied directly by the USB interface since the total current drawn by the circuit is a fraction of the USB 500 mA limit.



(a)

(b)

Figure 20 DAQ Module A. (a) General view; **(b)** Inner side; 1- Electrocardiograph circuit; 2- NI USB-6008©.

Since the signals obtained with this module and the SLP presented high levels of noise, this system was not used for CTs but only for lab trials.

5.3 Module B

A photograph of module B, the DAQ module's second version, is shown in figure 21.

It contains not only three different information channels arising from the integration of the SLP, the electrocardiograph circuit and one PZ transducer amplification circuit, but also the NI DAQ-6008© and the power supply.



Figure 21 DAQ Module B.

1-Electrocardiograph circuit; 2- NI USB-6008©; 3-PZ amplification circuit; 4- Accelerometric probe's input; 5-Power Supply.

The electrocardiograph circuit is identical to the one previously described.

The PZ transducer was included since it provided the means for the pressure wave detection and it would represent another important reference to the accelerometric signal. In order to extract its signal it was employed the same principle seen in HP's PZ [1], i.e. an IA (INA111²⁶) with current feedback via two 1M resistors, which was then followed by a TL081 and an OPO7CP inverting op amps. The full circuit schematic can be consulted in the Appendix B.

Since the USB power supply (a switching type) was found to be a major contributor to the noise level in module A, it was replaced by a linear power source, whose general scheme is described in figure 22.

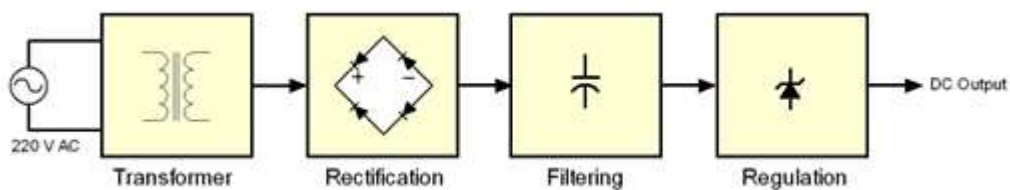


Figure 22 Block Diagram of the linear power supply design.

DC output = $\pm 5V$.

Due to its features, this system was taken to the IIFC for one month, in order to perform the first clinical data acquisition in hypertensive patients.

5.4 Module C

After placing the previous instrument in operation at IIFC, a third version of the module was developed. The main purpose of which was to use the Complior's® operating principle to measure the aortic PWV and, in the limit, to validate the accelerometric signals.

As a consequence, two PZ transducers were integrated, to be positioned in the classic sites: the carotid and femoral arteries. Their electronic circuit, shown in Appendix B, is based on INA126²⁷ IA also with current feedback, and the TL082 as an inverting op amp for delivering the output signal.

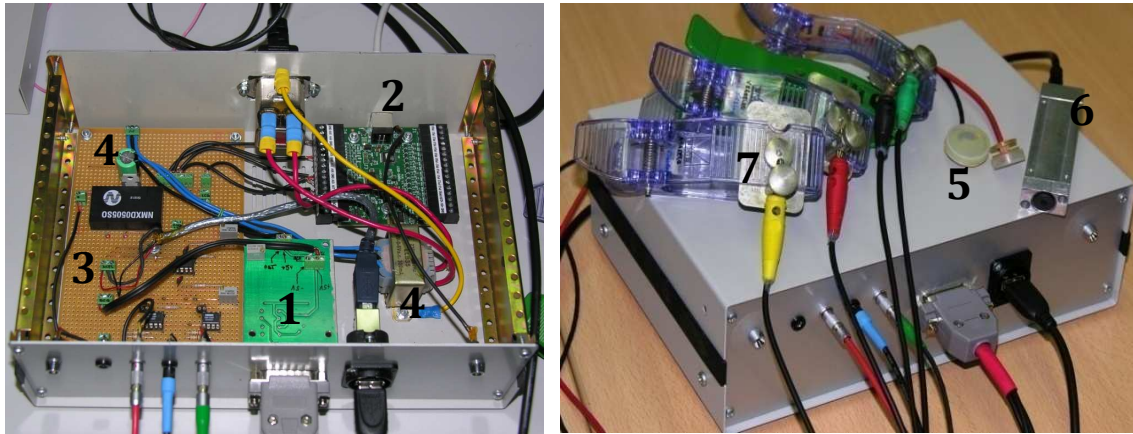
Together with the new information channel this module also included the SLP, the electrocardiograph circuit, the NI USB-6008© and a linear power source. The internal and external arrangement of module C can be seen in figure 23.

For two months, this instrument replaced the previous one at IIFC, where further CTs in patients with hypertension were carried out.

²⁶ The gain was set to $\approx 1,4$.

Data sheet at: <http://focus.ti.com/lit/ds/symlink/ina111.pdf>.

²⁷ The gain was set to 13.



(a)

(b)

Figure 23 DAQ Module C.

1-Electrocardiograph circuit; 2- NI USB-6008©; 3-PZ amplification circuit; 4- Power supply; 5-PZ Transducers; 6-SLP; 7-ECG electrodes.

5.5 Module D

The construction of the fourth DAQ module version, module D, was motivated by two distinct needs: 1) to cope with the development of bench models on lab, which could simplify the comprehension of clinical data; and, 2) the beginning of additional scientific research on PZ based pulse wave assessment.

As is displayed in figure 24, this module reproduces the architecture of module C, presenting the same three information channels (ECG, accelerometric and PZ), the NI USB-6008© and the linear power source.

In fact, the only difference between them is the gain associated to the PZ circuit ($G_D=5$) which, in module C, was causing signal saturation due to its high value ($G_C=13$).

For this reason this module and the recently made DP were taken to IIFC, where they have been in operation acquiring data up to today.

**Figure 24 DAQ Module D.**

1- ECG's input; 2- DP's input; 3-PZ circuit.

5.6 Module E

In order to accomplish all the requests previously described, module C was slightly modified, giving rise to the fifth and last DAQ module version: module E (figure 25).

The first improvement had to do with the gain of the PZ, which was adjusted to the gain of module D. Besides, the two current amplifiers INA126 were replaced by two INA114.

The second upgrade consisted in the insertion of a pressure acquisition channel that would be employed in the developed bench models (see Chapter 7). The pressure sensor used was the HCXM100D6V²⁸.

At last, the main similarities and differences between each module are resumed in table 5.



Figure 25 DAQ Module E.

1- Pressure sensor's input; 2- HP's input

Table 5 Summary of the developed modules and its main features.

Features Modules	Measurement Probe Incorporated	ECG	No. of Piezos	Function	Others
A	SLP	✓	×	Trial Run	Switching Power Source (USB)
B	SLP	✓	1	CTs	Linear Power Source
C	SLP	✓	2	CTs	Linear Power Source
D	DP	✓	2	CTs	Linear Power Source
E	HP	✓	2	Pulsatory Model	<u>Pressure Channel</u> Linear Power Source

References

[1] Wuchinich, Dave. "Circuit suppresses capacitively coupled noise pickup by the piezoelectric sensor and its wiring." *EDN: Design ideas* 23 11 2006 75-76. 15 Aug <http://www.edn.com/article/CA6391432.html>

²⁸ Differential pressure range: 0-100mbar;

Data sheet at: <http://www.lascarelectronics.com/DATA/sensor/HCX005D6V.pdf>.

CHAPTER 6

ACCELEROMETER CALIBRATION

Prior to the clinical experiments with the differential probe, two bench models were developed in order to help to interpret the clinical data.

The first model relates to the calibration of the accelerometer, while the second one has to do with the simulation of a pulsatory system for the full understanding of the relationship between accelerometric, PZ and pressure signals (Chapter 7).

This chapter focuses only the calibration of the accelerometer, firstly by describing the experimental set-up and, afterwards, by interpreting the obtained results.

6.1 Introduction

As mentioned in chapter 2, the calibration process consists in applying an excitation or a reference signal of known mechanical characteristics and measuring the subsequent electrical output of the sensor/instrument under test ^[1].

To achieve this goal, we made an option of building a slider-crank mechanism (SCM), due to its simplicity and ease of construction. Through this reference apparatus, a sinusoidal-like motion, with variable frequencies and amplitudes is produced to measure the ADXL203 accelerometer output.

In order to understand the basic concepts of a SCM, the next subsection is entirely devoted to its mathematical description.

6.1.1 Slider-Crank Mechanism

The SC mechanism is an arrangement of mechanical parts designed to convert rotary motion to straight-line motion or vice-versa.

The basic nature of the mechanism and the relative motion of the parts can be best described with the help of figure 26.

The darkly shaded part 1 corresponds to the cylinder²⁹, in which the piston or slider (part 4) slides back and forth. The crank, part 2, is shown as a straight line member extending from

²⁹ Or two guides.

the bearing at *A* to the bearing at *B*, which in turn attaches it to the connecting rod, part 3. The small circle at *A* is the main crankshaft bearing [2] [3].

The connecting rod is shown as a straight member extending from the bearing at *B* to the bearing at *C*, which connects it to the piston.

Thus, these three bearings, shown as circles at *A*, *B*, and *C*, permit the connected members to rotate freely with respect to one another [3].

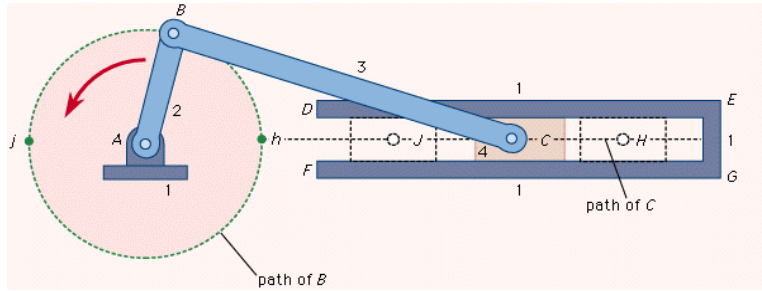


Figure 26 Crank Mechanism.

A- Crankshaft; **AB-**Crank; **BC-** Connecting rod; **C-**Slider or piston.
Adapted from [2].

The path of *B* is a circle of radius *AB* and the path of *C* is a segment of length *JH*. When *B* is at point *h* the piston will be in position *H*, and when *B* is at point *j* the piston will be in position *J*.

Piston Motion Equations

The piston describes an oscillatory movement which can be approximated to the simple harmonic movement (SHM) when $\overline{BC} \gg \overline{AB}$ [3].

The mathematical equations which express the position, velocity and acceleration of the piston are summarized in table 6 and represented graphically in figure 27. For further reading refer to [3] [4] [5].

Table 6 Comparison between piston motion and SMH equations [3] [4].

	Piston's Movement	SHM
Position (x)	$r\cos(wt) + \sqrt{l^2 - r^2} \sin^2(wt) - \sqrt{l^2 - r^2}$	$r\cos(wt)$
Velocity (v)	$-rwsin(wt) \cdot \left[1 + \frac{r \cos(wt)}{\sqrt{l^2 - r^2} \sin^2(wt)} \right]$	$-rwsin(wt)$
Acceleration (a)	$-rw^2 \cdot \left[\cos(wt) + \frac{r(l^2 \cos(2wt) + r^2 \sin^4(wt))}{(l^2 - r^2 \sin^2(wt))^{\frac{3}{2}}} \right]$	$-rw^2 \cos(wt)$

Notation: Crank radius= \overline{AB} = *r*; Crank's constant angular velocity=*w*; connection rod's length: \overline{BC} = *l*

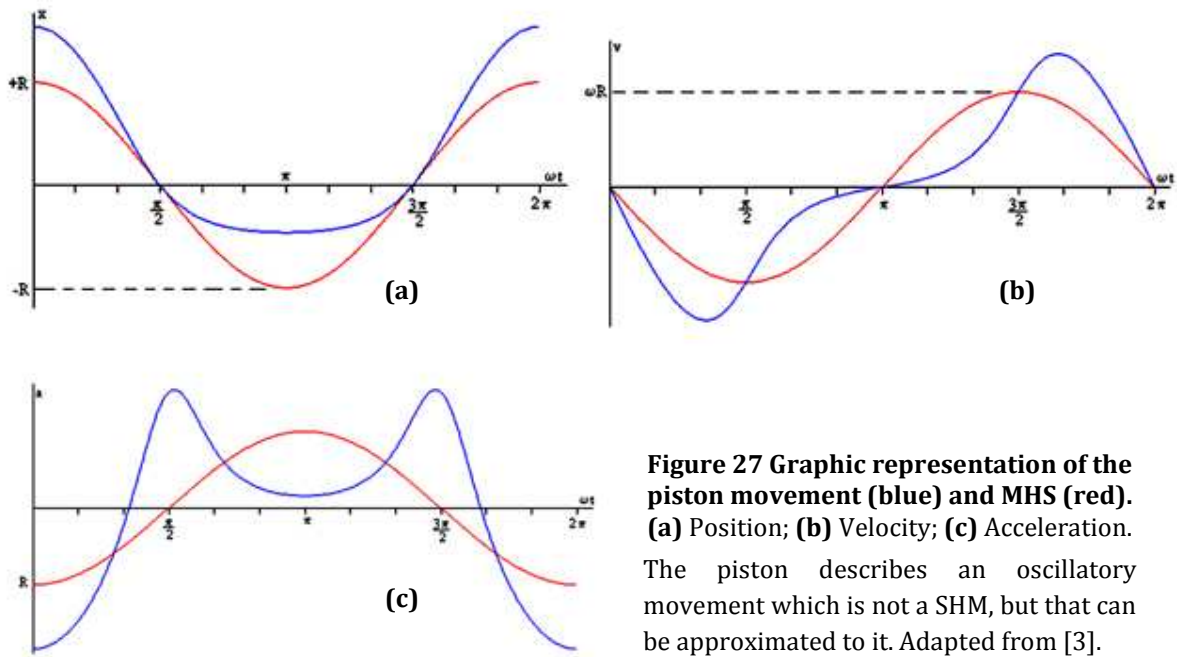


Figure 27 Graphic representation of the piston movement (blue) and MHS (red). (a) Position; (b) Velocity; (c) Acceleration.

The piston describes an oscillatory movement which is not a SHM, but that can be approximated to it. Adapted from [3].

6.2. Methods

6.2.1 Experimental Configuration

Figure 28 shows an overall view of the bench model developed for the accelerometer calibration.

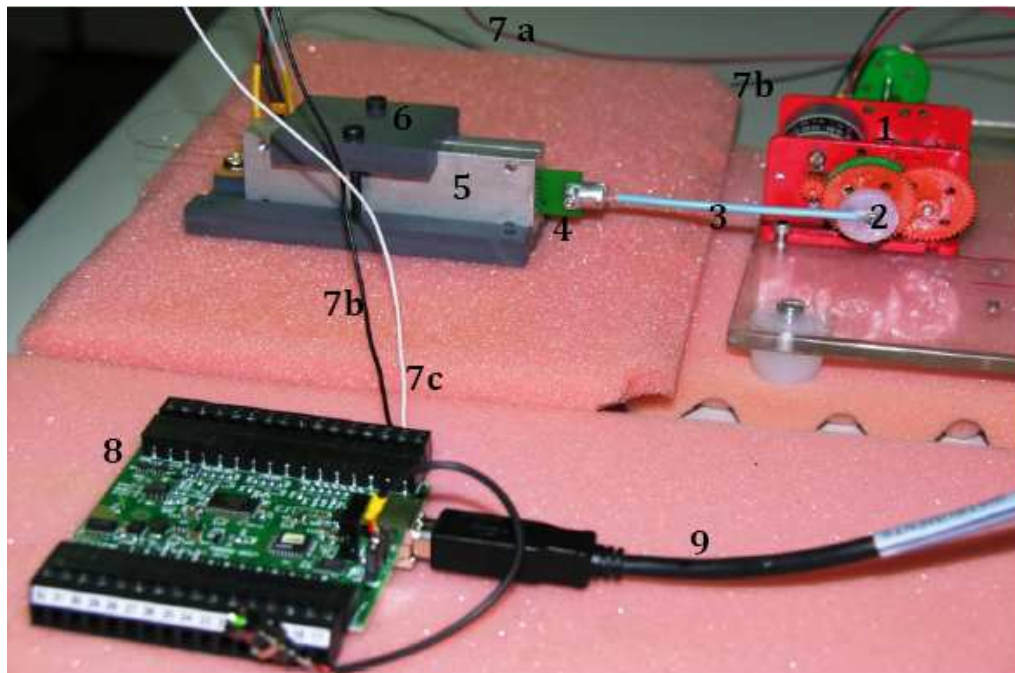


Figure 28 Experimental set-up of accelerometer calibration.

1-Brushed DC motor; 2- Crank 3- Connecting rod; 4-PCB holding AXL203CE Accelerometer (piston); 5- Probe's metal body; 6- Probe's support piece; 7- Connection wires: a) +5V, b) Ground; c) Signal; 8- NI USB-6008©; 9- USB Cable.

The calibration system was basically constituted by the SC apparatus, the DAQ module NI USB-6008© and the power sources.

To perform, the SC mechanism, the brushed DC motor and the probe's main covering were respectively fixed in acrylic and PVC surfaces. The electronic circuit³⁰ (piston) was placed in the inner side of the probe (cylinder) and connected to the motor's shaft (crankshaft) by a copper wrapped wire (connecting rod).

It was also placed a cog wheel (crank) with different eccentricities (3mm, 4mm, 5mm and 6mm) on the top of motor's geared shaft, in order to obtain different piston's displacement amplitudes. The DC motor was powered by variable voltage so that different frequencies could be obtained.

When this mechanism was set in motion, the accelerometer output was sampled at a 1k samples per second (sps), during 60s.

6.2.2 Experimental Measurements

Two experiments were made in order to achieve the accelerometer calibration.

Experiment A consisted on the verification of the quadratic law associated to the acceleration of the electronic circuit ($a = -r\omega^2 \sin(\omega t)$). Thus, in the first set of measurements, the cog wheel eccentricity was set to its maximum (6mm) and the system's angular velocity was successively increased by stepping up the motor's supply voltage. The various accelerometer outputs were then recorded.

Experiment B was aimed at obtaining the accelerometer curve calibration, i.e., the relation between the peak voltage of the accelerometer and the peak acceleration of the piston. In this set of measurements, the system's angular velocity was kept constant (constant motor supply) while the amplitude of the oscillatory movement was changed by increasing the cog wheel eccentricity.

6.3 Results and Discussion

6.3.1 Experience A

Verification of the quadratic law associated to SHM

In a first approach, it was attempted to explore the quadratic law associated to the SHM. Since the results were not clear, they won't be presented.

³⁰ PCB with the AXL203CE accelerometer.

6.3.2 Experience B

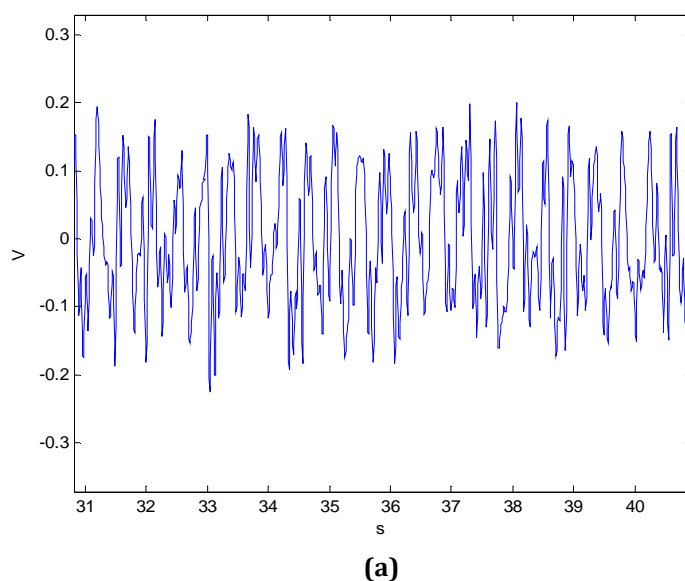
Determination of the calibration curve

In order to get the calibration curve of the accelerometer, several sets of accelerometer data were acquired.

Data analysis (Matlab®) consisted in the following steps:

- 1: File loading and visualization;
- 2: Band-pass filtering of data;
- 3: Fast Fourier Transformation (FFT) of data;
- 4: Visualization of the amplitude spectra,

Figures 29(a) and 29(b) show a typical output signal obtained from the ADXL203 as well



as its amplitude spectra.

In these two types of graphics, we intended to extract the peak voltage from the accelerometer (graphic a) and the fundamental frequency associated to its movement (graphic b).

In the amplitude spectra, it was compared the value of the fundamental frequency with the respective system's oscillation frequency, given by the motor's rotation. As expected, the both values were in agreement³¹.

The presence of another harmonics in this spectrum suggested, straight away, that the movement of the SC apparatus was not closer to the pure SHM.

Concerning the graphic of accelerometer's output, it was necessary to find a strategy to extract the peak voltage, since the accelerometer's output signal presented high levels of noise, even after filtering.

In order to obtain this peak, it was made an approximation which consisted in to situate, along the acquisition file, a pattern of two peaks similar to the figure 27(c) and then to make a mean of all these peaks. This assumption was based again in the fact that the system movement was not pure simple harmonic.

³¹ The rotations per minute for a determined tension are tabled in the motor's data sheet. In this experience, the tension applied to the motor was of 3V and consequently the motor's rotation should be of 2.4Hz (real value), which is in agreement with the obtained in figure 2 b (≈ 2.342 Hz).

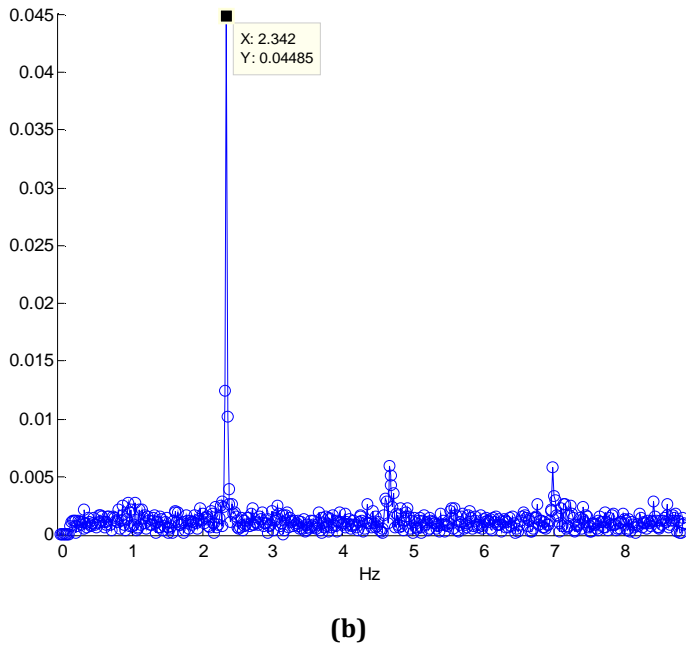


Figure 29 Data Pre Processing
(a) Filtered output signal of the ADXL203 accelerometer,
(b) Amplitude spectre.
 Both signals were obtained by the application of the program developed in Matlab®.

Table 7 is based on the previous conjecture and resumes the values of peak voltage and peak acceleration determined for the different oscillation amplitudes of the SC system.

The calculation of the peak acceleration values was based upon equation 4. This equation corresponds to the absolute maximum of the piston’s movement acceleration expression (table 6) [5].

$$a_{max} = w^2 r (1 + \frac{r}{l}) \quad \text{(Eq. 4)}$$

In this experience, w is a constant equal to 2,342Hz, r is the amplitude (equal to the eccentricity) and l (connecting rod’s length) is also a constant equal to 0,069m.

Table 7 Amplitude, peak voltage and peak acceleration values

Amplitude (m)	Peak Acceleration (m/s ²)	Peak Voltage (V)
0,006	3,180	0,213
0,005	2,588	0,151
0,004	2,020	0,114
0,003	1,477	0,089

The respective calibration curve obtained is shown in figure 30.

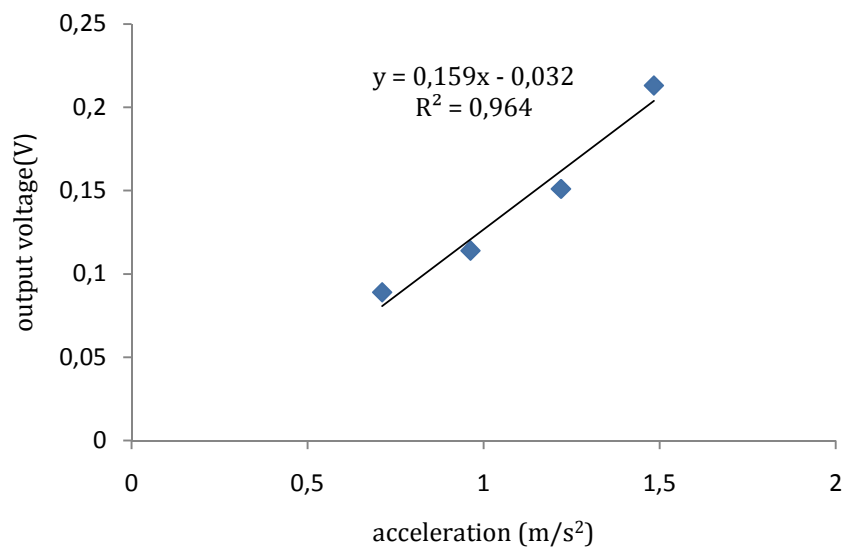


Figure 30 Accelerometer's Curve Calibration

The measured sensitivity of the accelerometer is therefore $0,159\text{V}/\text{m}\cdot\text{s}^2$ (the curve's slope).

Since the manufacturer's stated sensitivity on the accelerometer's data sheet is $1\text{V}/g=0,102\text{ V}/\text{m}\cdot\text{s}^2$, it is possible to determine the measurement error, defined as the difference between the measured value and the true value of the measure:

$$E = |(measured) - (true)| = 0,057$$

6.4 Conclusions

The developed slider-crank mechanism did not reveal itself as a good option for accelerometer calibration, since the error between the measured sensitivity and manufacturer's stated sensitivity was high and it seems to proportionate only a small fraction ($1/17$) of the accelerometer's measurement range ($3,4\text{ g}$).

The principal causes for the measurement error must be associated not only to the experimental set-up but also to the data acquisition and processing.

Regarding the experimental set-up, the poor SNR of the calibration data derives from noise originated by: 1) motor brushes, 2) lack of stiffness of the connecting road, 3) breadth in the articulations (mainly between the connecting road and the crankshaft bearing, 4) external shakings due to the poor of isolation of the system and also 5) possible friction inside the probe's body.

On the other hand, and in what concerns data acquisition and processing, the approach to estimating the peak voltage by directly reading the peak values in the accelerogram, was

probably not adequate, since it is subjective. Thus, the future utilization of this mechanism in accelerometer calibration would necessarily imply an optimization of the experimental configuration, in order to obtain higher SNR, and would also require second thoughts on data processing methods. Eventually, the exploitation of the singularities of the spectral properties of functions x_x, y_y , will lead to interesting results.

References

- [1] Webster, John G., *Measurement, Instrumentation and Sensors Handbook*, 1st ed. New York: CRC Press LLC, 1999, pp:
- [2] "Slider-crank mechanism." Online Art. Encyclopædia Britannica Online. 3 Sept. 2007 <http://www.britannica.com/eb/art-7447>
- [3] García, Ángel. "Movimiento de un pistón." *Física con ordenador*. 3 Oct 2006. 2 Sep 2007 <http://www.sc.ehu.es/sbweb/fisica/oscilaciones/biela/biela.htm>
- [4] "Piston motion equations." 7 Jul 2007. Wikipedia. 2 Sep 2007 http://en.wikipedia.org/wiki/Piston_motion_equations
- [5] Santos, António, "Introdução aos motores de combustão interna", Class Notes, pp.15-17

The pulsatory model is divided in two main parts: the fluid circulation circuit and the DAQ system.

The fluid circulation circuit is fixed on an acrylic surface and is constituted by plastic tubes, a water reservoir (500 ml), a peristaltic pump (PP)³² and a 10 mA differential circuit breaker, which protects the operator from over load or short circuit, and powers up motor pump. The PP establishes a water pulsatile flow of 5l/h in the direction of the arrows, as the figure points out.

The DAQ system comprises the HP, the HCXM100D6V differential pressure sensor and the module E. The HP, horizontally fixed with an appropriate holder, is leaned against a rubber elastic membrane. The need to glue an elastic membrane on the plastic tube is due to its stiffness, which would make difficult the signal acquisition. Previously to gluing the rubber elastic membrane to the tube a partial small cut have to be done.

7.2 Results

With the configuration described before it was possible to acquire accelerometric, PZ and pressure signals, simultaneously.

In figure 32 is shown the **typical signals** obtained during 4s, using an acquisition sample rate of 1ksps. These signals were already filtered in Matlab® with a band-pass filter of [0.4 Hz, 45 Hz].

7.3 Data Processing

The acquired signals suffered a very superficial data processing treatment, however, and having in mind to find a relationship between the patterns recognized for each signal, the accelerometric and PZ signals were compared.

It was developed a small algorithm which consisted in the following main steps and whose final result is presented in figures 33(a) and 33(b):

Step 1: File load and visualization;

Step 2: Filtering: application of a band-pass filter [0.4 Hz, 45 Hz];

Step 3: Double differentiation of the PZ signal;

Step 4: Normalization of the accelerometric and the differentiate PZ, signals;

Step 5: Simultaneous visualization of the normalized signals.

³² A peristaltic pump is a type of positive displacement pump (compression pump) used for pumping a variety of fluids. The fluid is contained within a flexible silicon tube fitted inside the circular pump casing. A rotor, with a determined number of rollers, compresses the flexible tube in order to produce the flow. For further reading: http://en.wikipedia.org/wiki/Peristaltic_pump2

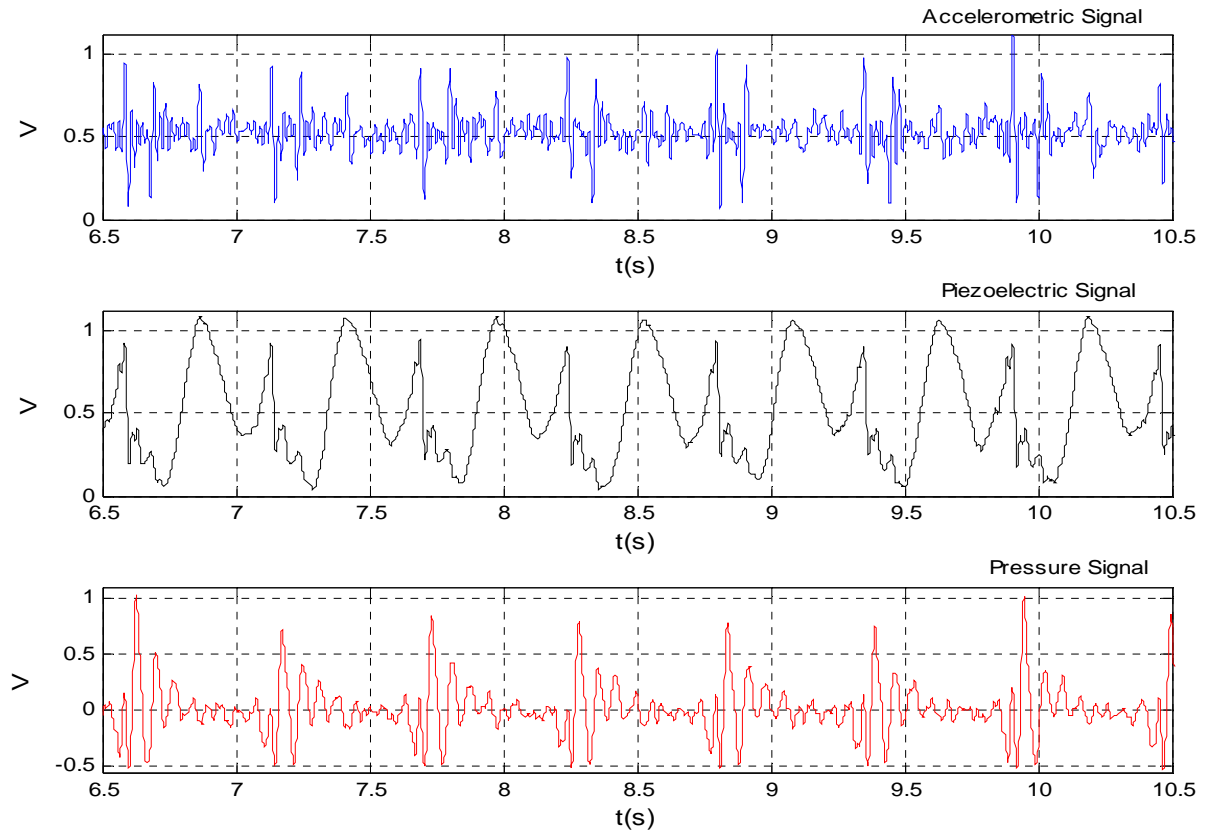
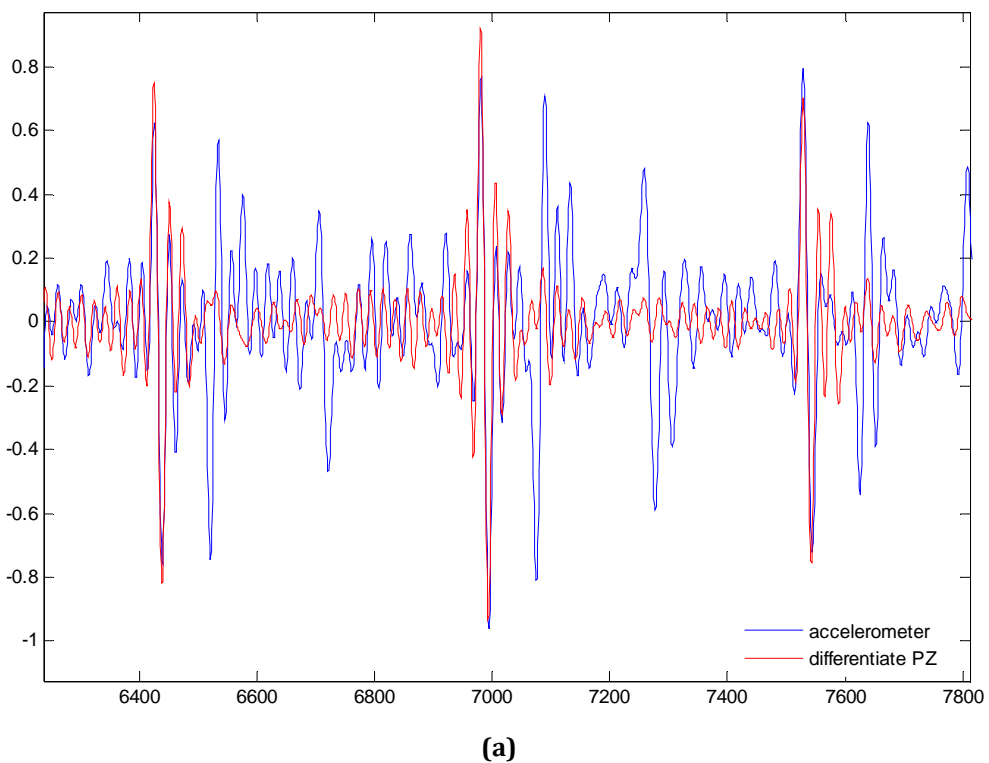


Figure 32 Accelerometric, PZ and pressure signals acquired in the pulsatory model during 4s.



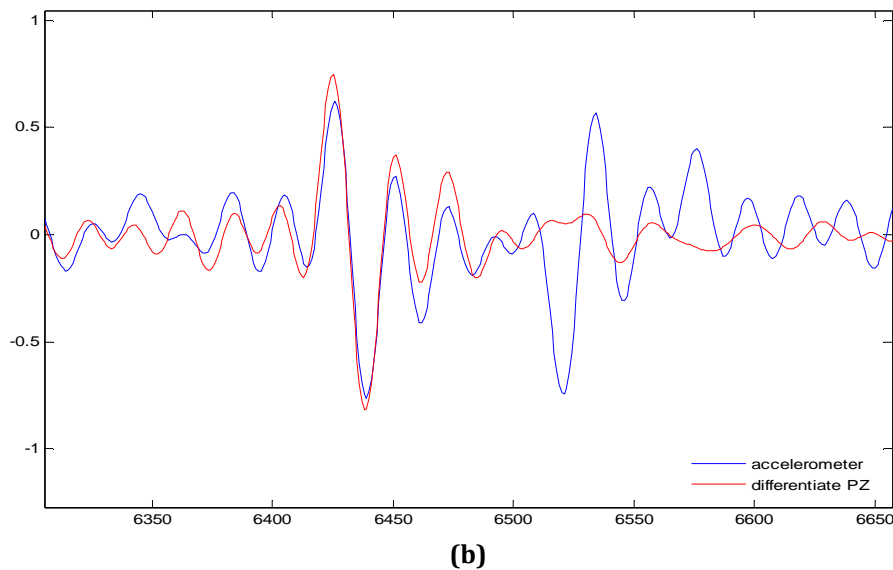


Figure 33 Accelerometric and Double Differentiate PZ Signals:
(a) General view. **(b)** Peak amplification.

It is observed an explicit correlation between the shapes of both signals. Thus, it is proved that the accelerometer gives, **at least**, the same information as the PZ when it is differentiated twice. In fact, we suppose that the information provided by the accelerometer can be more valuable than those obtained directly by the PZ, since PZ is inherently an AC coupled device and, as such, its frequency response always depends on the time constant of the overall circuit, and it is inevitably impaired in the very low range (DC to 0.2 Hz), where a number of auto-regulatory effects of the human body, are located [1].

Moreover, even for the frequencies where the response is not affected by the coupling (0.2 Hz up to resonance), the response delivered by PZ is affected by the way the operator holds the probe and presses it against the region under test (this is the reason why the HP has been fixed in this model). This uncertainty is due to the complex relationship between charge polarization and externally applied forces in the bulk of the sensor material.

For these reasons PZs cannot be calibrated in terms of a mechanical unit (pressure, force, torque or other) against output voltage. In fact all hemodynamic instruments using PZs are used for time measurements, only.

Accelerometers, on the contrary, are truly DC devices capable of a complete 3-axis assessment of a precise mechanical parameter, and when incorporated in a well designed probe, many artefacts, associated to the operator involuntary movements, can be eliminated.

References

[1] Humeau, Anne. et al, Numerical Simulation of Laser Doppler Flowmetry Signals Based on a Model of Nonlinear Coupled Oscillators. Comparison with Real Data in the Frequency Domain (I), Proceedings of the 29th Annual International Conference of the IEEE EMBS, pp. 4068-4071.

CHAPTER 8

CLINICAL RESEARCH TESTS

This final chapter describes the procedures of the CTs carried out in IIFC, and establishes a comparison between the data acquired with the various probes/modules.

8.1 CTs Procedures

As mentioned before, the second period of CTs was carried out respectively by: the SLP/module B (1 month), the SLP/module C (2 months) and the DP/module D (in still progress).

The clinical trials **main** objective is to **explore** the **potential** of the **accelerometer** based probes in the assessment of PWV, by comparing their information with the one of a standard method (Complior®). Since the DAQ modules C and D incorporate a similar (and inexpensive) input, based on a principle similar to the Complior's®, it is also intended to investigate the feasibility of extracting transit time curves with this platform, to further PWV computing.

The type-of-patient criteria of selection changed in relation to the first period (section 3.3.1): currently, all patients are **hypertensive** and have been submitted to drug treatment. This circumstance makes it possible a valuable comparison of PWV values, before and after medication.

The three types of acquisitions performed are summarized in table 8.

Table 8 Acquisition types performed with the various probes/modules.
(It was used the Complior® to perform a 4th test, in order to obtain the PWV real value).

<i>Acquisition Type</i>	<i>Description</i>
Probe + ECG	After the ECG sensors are located in agreement with lead I configuration, the operator places the measurement probe over the carotid artery, during 30-45s.
Probe + PZ	Two operators place the probe and the PZ, respectively, in opposition over the carotid arteries, during 30s-45s.
PZ + PZ¹	The operator places the PZs over carotid and femoral arteries during 15 s, approximately.

¹The PZ+PZ CT was not performed by the SLP/module B.

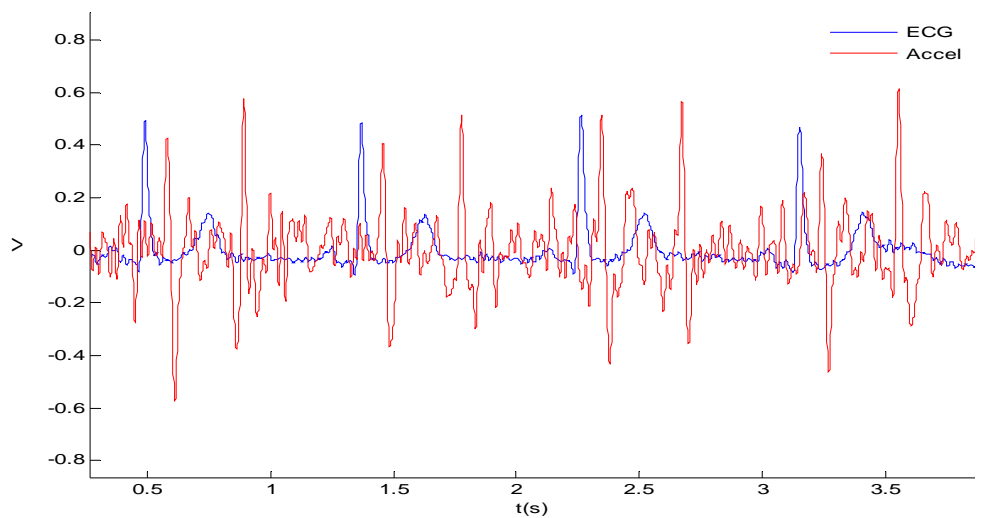
8.2 Data Pre-Processing

Up to now, data from nearly forty patients have been subject to the clinical trials and some of them are now entering the second turn of evaluation.

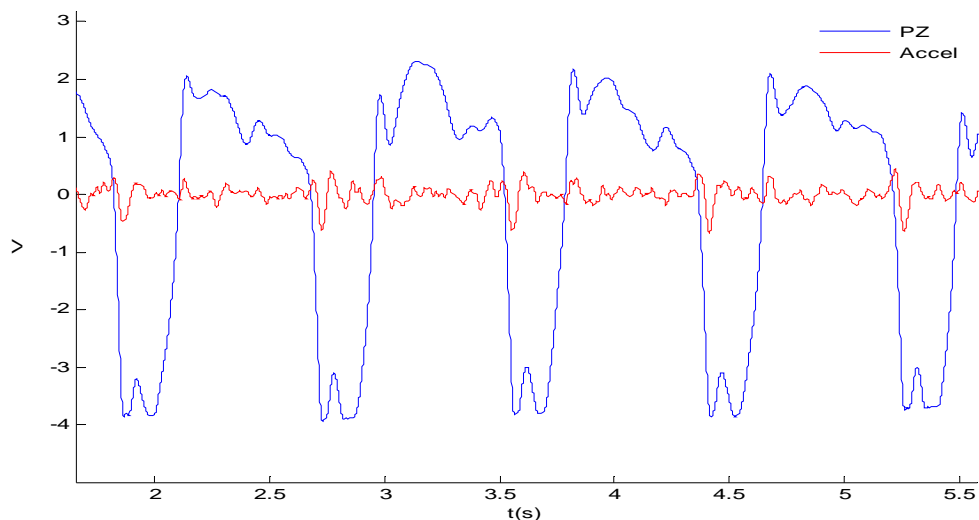
However, and since the **project's priority** was **hardware optimization** in order to obtain **signals** with **high SNR**, the acquired data has not yet been processed, in an attempt to relate them with the Complior's® information. In fact, so far, the data pre-processing that was carried out (data visualization and filtering) has been used for the instrument improvement, only.

Next, some representative examples are shown in order to compare signals obtained with the different instrument set-ups (figures 34, 35 and 36).

1) SLP/Module B



(a)



(b)

Figure 34 Signals acquired by the SLP/Module B in one patient.

(a) ECG+Accelerometer. (b) ECG+PZ.

2) SLP/Module C

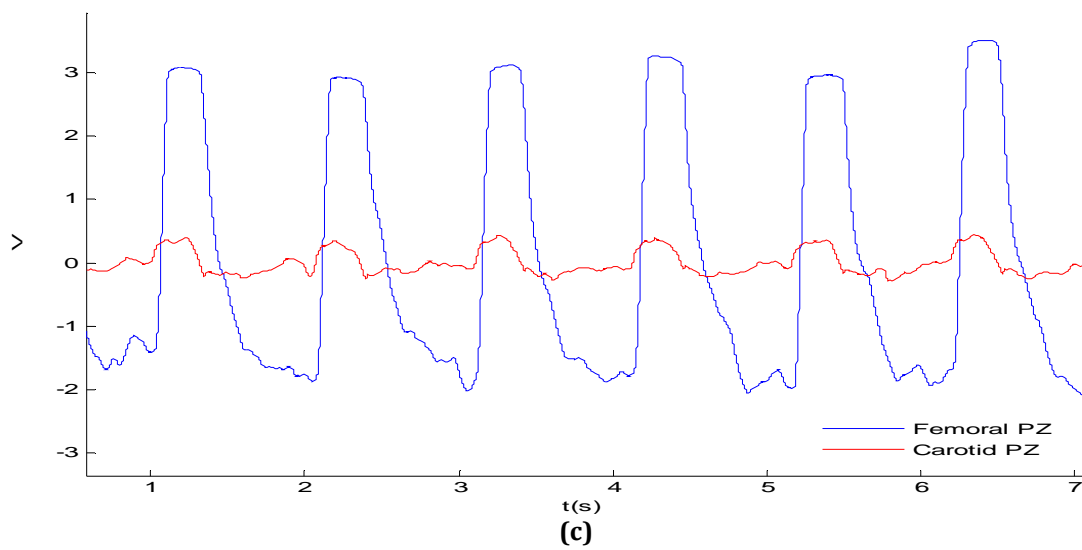
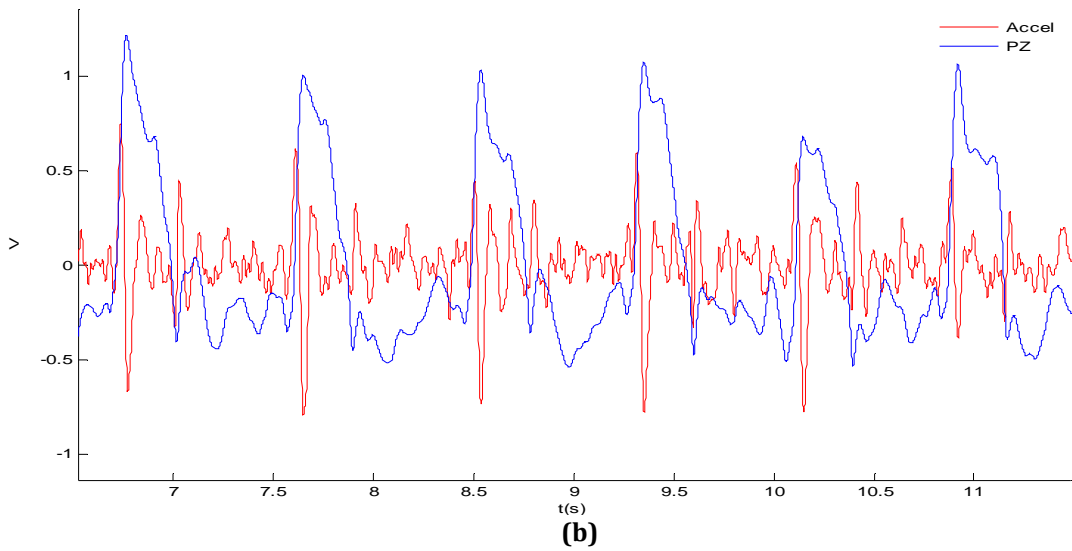
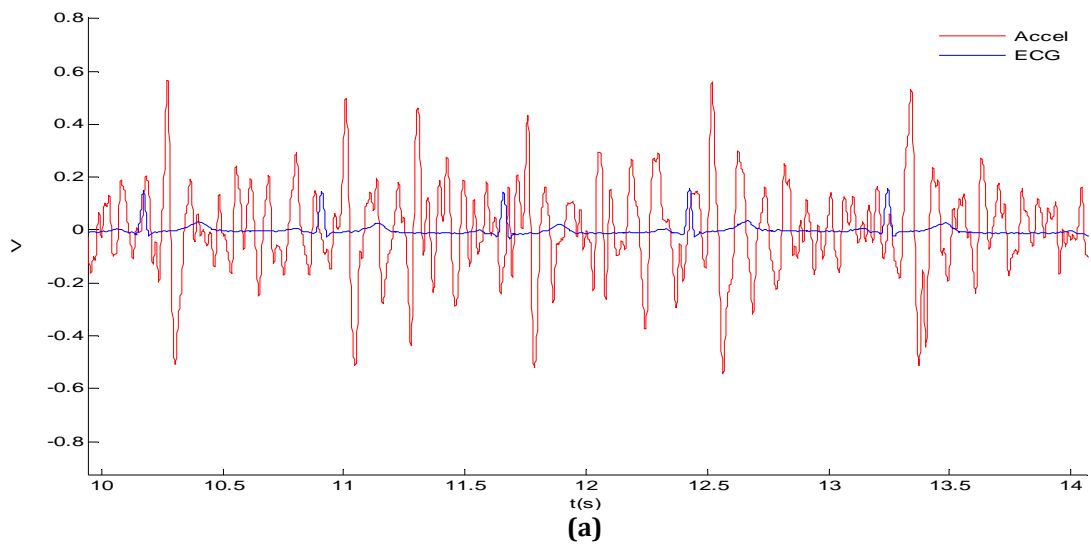


Figure 35 Signals acquired by the SLP/Module C in one patient. (a) ECG+Accelerometer. (b) ECG+PZ. (c) Carotid PZ+ Femoral PZ.

3) DP/Module D

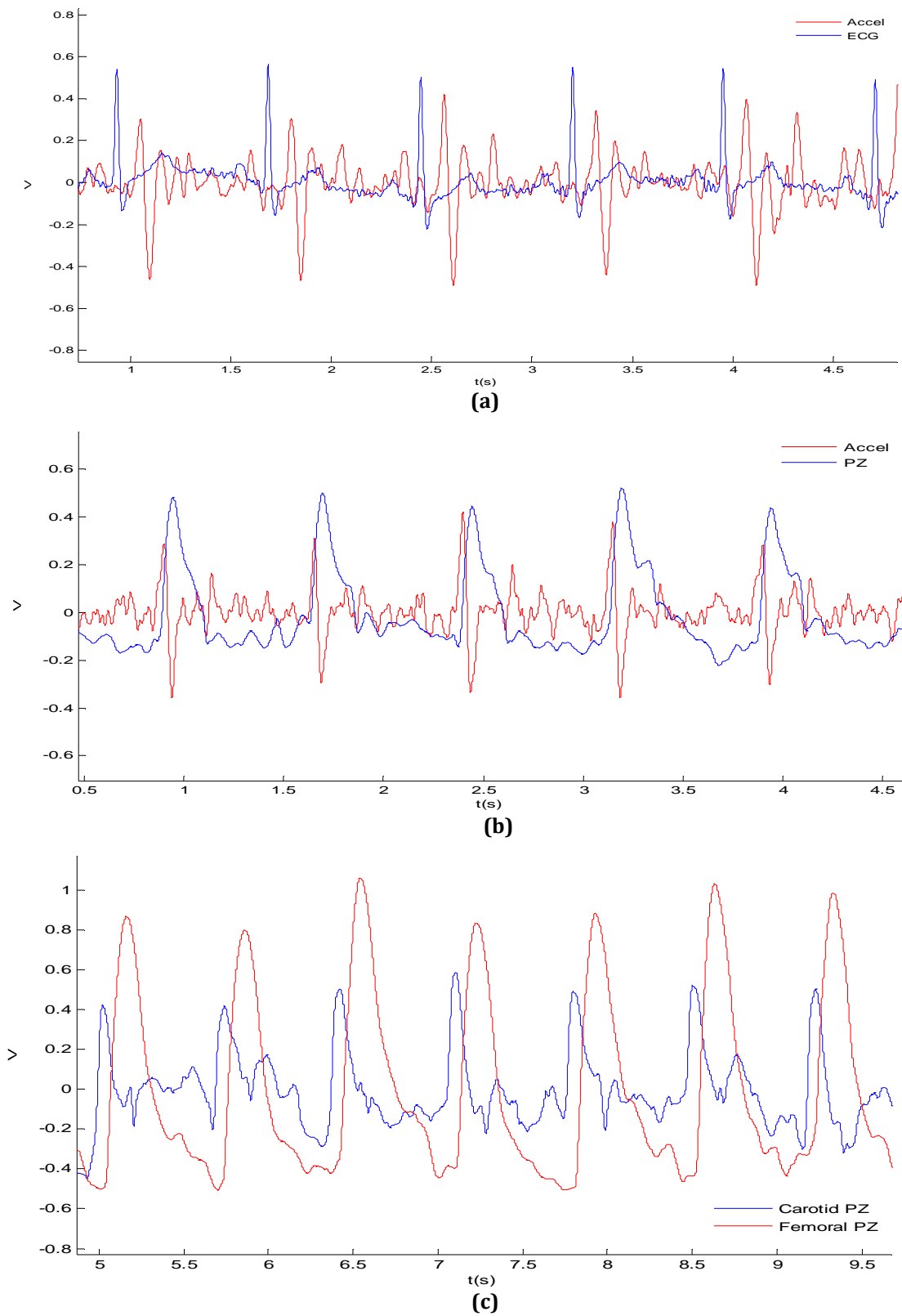


Figure 36 Signals acquired by the DP/Module D in one patient. (a) ECG+Accelerometer. (b) ECG+PZ. (c) Carotid PZ+ Femoral PZ.

It is quite clear that the accelerometric and PZ signals acquired with the DP/module D set-up exhibit higher SNR than those obtained with the other probe/modules set-ups, and the observed saturation on PZ signals has disappeared also when using this set-up. In fact, the only signals whose SNR is constant throughout the use of different set-ups are the ECG ones.

Although the pre-processing of the clinical data is not enough to conclude the exact information values that the accelerometer is able to give, the existence of very well defined correlations between the different signals is also very clear, thus making it an interesting subject for further research.

CHAPTER 9

CONCLUSIONS AND FUTURE WORK

Once the project's academic component has been achieved, it is now necessary to evaluate and discuss the work that has been done, the results obtained and the future developments.

9.1 Conclusions

The main objective of this project was the development of instrumental methods, based in accelerometry, for PWV hemodynamic characterization.

Three accelerometer based probes (SLP, DP and HP) and five multisensor DAQ modules (A, B, C, D and E) were designed and built for this purpose and have been tested in the field.

In its research usage, they have proved effective in the prolonged follow up of hypertensive patients and, at this point, the instrument with the better performance is the DP and module D, which exhibit signals with a higher SNR.

The pre-processing of the clinical data was not conclusive about the exact information that accelerometer was able to give, but the existence of very well defined correlations between the ECG, accelerometric and PZ signals suggests a high potential for this new technique.

In order to help the comprehension of the clinical data, two bench models were also developed. The first addresses the calibration of the ADXL203 accelerometer. Although the simplicity of the mechanism was very attractive, the device was only capable of testing a small fraction of the accelerometer's measurement range. In addition, the difference between the measured sensitivity and manufacturer's stated sensitivity was extremely high.

The second model had to do with the simulation of a pulsatory model. The analysis of the signals acquired with the HP revealed that the accelerometer delivers, at least, the same information as the PZ when its output curve is differentiated twice.

In the future, it is expected that the best performance in clinical trials would be from the HP or from a similar version, which, in the limit, will be able to compute PWV punctually in the carotid artery.

9.2 Future work

In this work, the feasibility of using accelerometers in the assessment of PWV was explored and the results obtained with prototype probes were indeed very promising.

However, there is still much work to be done in order to achieve a powerful and reliable instrument for hemodynamic characterization of PWV, and to turn this technique into a marketable technology.

Since this project is to be continued, the two main steps which are necessary to take in the short term are related not only to the instrument itself but to the clinical data processing.

Instrument Optimisation

Since they two major limitations on the performance of NI-DAQ 6008 © were found (software inflexibility and reduced real time capacities), it will be necessary to develop an electronic platform with real time signal analysis capacity. The integration of a late generation microcontroller as the unit's core will be the best solution.

The analog front end should maintain the current number of channels (accelerometric probe, PZ transducers, electrocardiograph circuit), but must have a modular structure to allow simple adaptations in order to add other sensors of interest (temperature, oximetry...). As for the communication with the PC, although not critical, it should be done by means of a standard RF communication protocol (Zigbee, Bluetooth...), in order to guarantee connectivity and portability.

The validation of this platform will be made with the clinical tests extension.

Clinical data Processing

Undoubtedly, clinical data processing is the key to the major goals of this work. It will remove the obstacles found in the assessment of PWV values obtained by accelerometry, and will enable a comprehensive comparison with Complior's® data.

Ultimately, it will be data processing that will lead the way to the validation of a clinical instrument based on the new (to our knowledge) techniques unveiled in this work.

To attain this goal, it will be necessary, firstly, to study the relationship between the different signals in an ideal model and, then, bring the data processing, already started for the pulsatory model, to a conclusion.

APPENDIX A

THEORETICAL ASPECTS

1. PIEZOELECTRIC SENSORS

PZ sensors, used in a variety of pressure-sensing applications, measure the electrical potential caused by applying mechanical force to a PZ material. PZ materials can be divided in two main groups: crystals and ceramics. The most well-known is quartz (SiO₂).

A PZ sensor is based on the PZ effect³³, in which energy is converted between mechanical and electrical forms. Specifically, when a polarized crystal is put under pressure, some mechanical deformation takes place in the polarized crystal, which leads in the generation of the electric charge.

There are many types of PZ sensors. Examples include a PZ accelerometer, PZ force sensors, and PZ pressure sensors. A PZ accelerometer is suitable for working at a lower power consumption and wider frequency range. PZ force sensors are low impedance voltage force sensors designed for generating analog voltage signals when a force is applied on the PZ crystal and are widely used in machines for measuring force. PZ pressure sensors are used for measuring change in liquid and gases pressure [31].

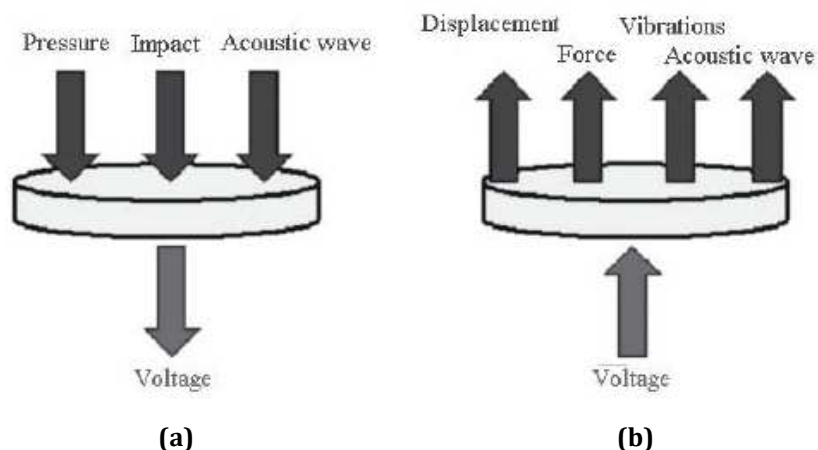


Figure 37 Functions of a piezoelectric sensor [30].

(a) Mechanical deformation --> Electrical Potential. **(b)** Electrical Potential --> Mechanical deformation.

³³ PZ effect was discovered in the 1880's by the Curie brothers.

2. ELECTROCARDIOGRAPHY

Heart's Anatomy

The next figure is a sketch of the heart, showing its main structures and arterial and venous connections:

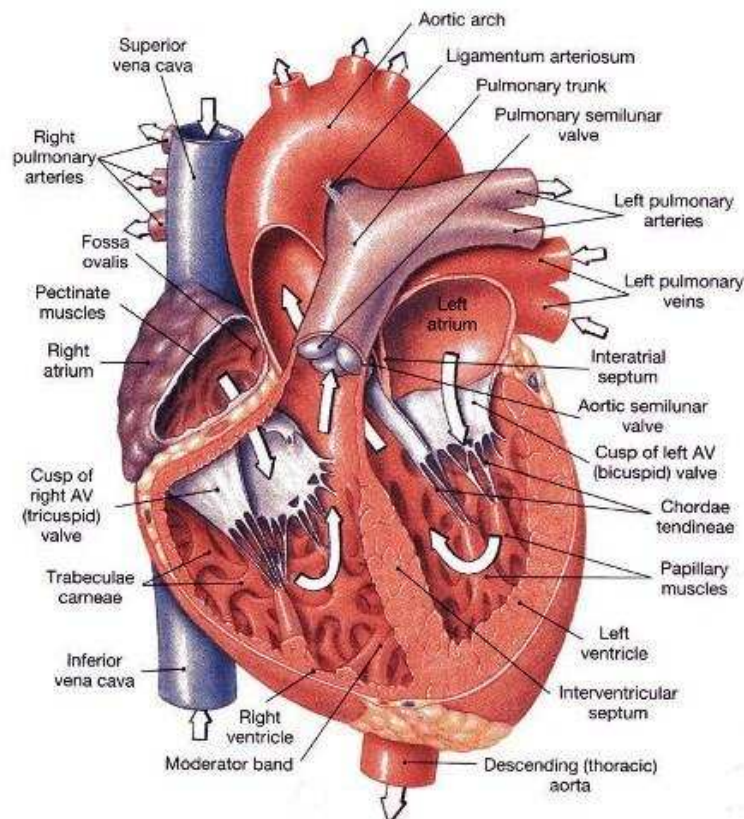


Figure 38 The Heart. Adapted from [25].

12-Lead Placement Diagrams

The 12-lead ECG provides spatial information about the heart's electrical activity. The three standard limb leads (I, II, III) and the augmented limb leads (aVR, aVL, aVF) detect the electrical potential change in the frontal plane. The six precordial leads (V₁, V₂, V₃, V₄, V₅, V₆), each in a different position along the chest, record the electric potential change in the heart in a cross sectional plane. The diagrams below illustrate the location of the electrodes for each lead.

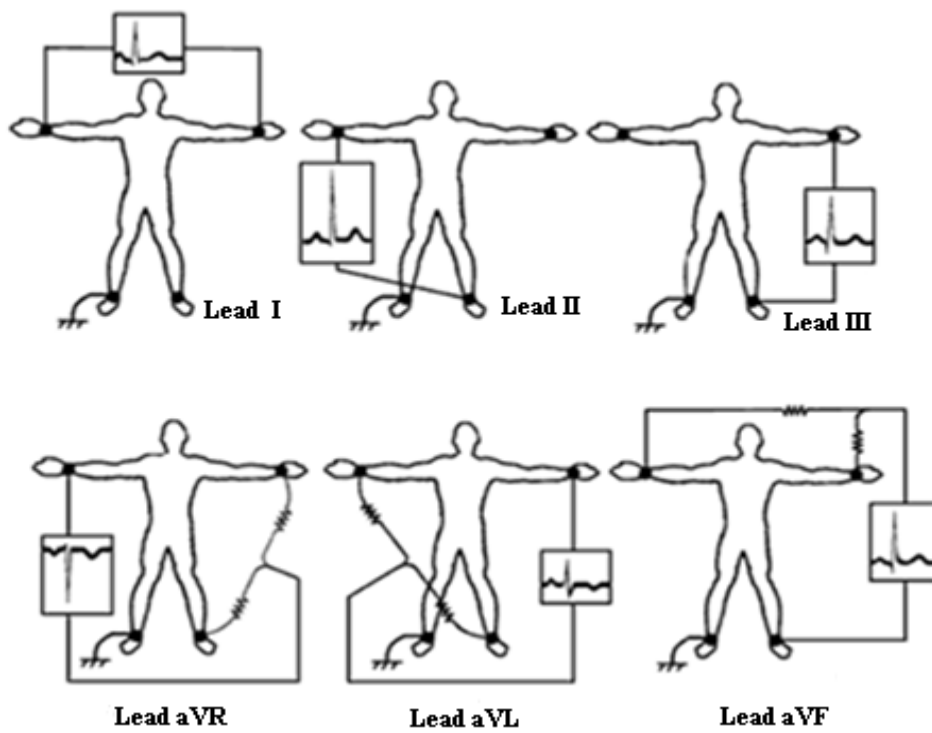


Figure 40: Location of the electrodes in the Standard Limb Leads and Augmented Limb leads. Adapted from [26].

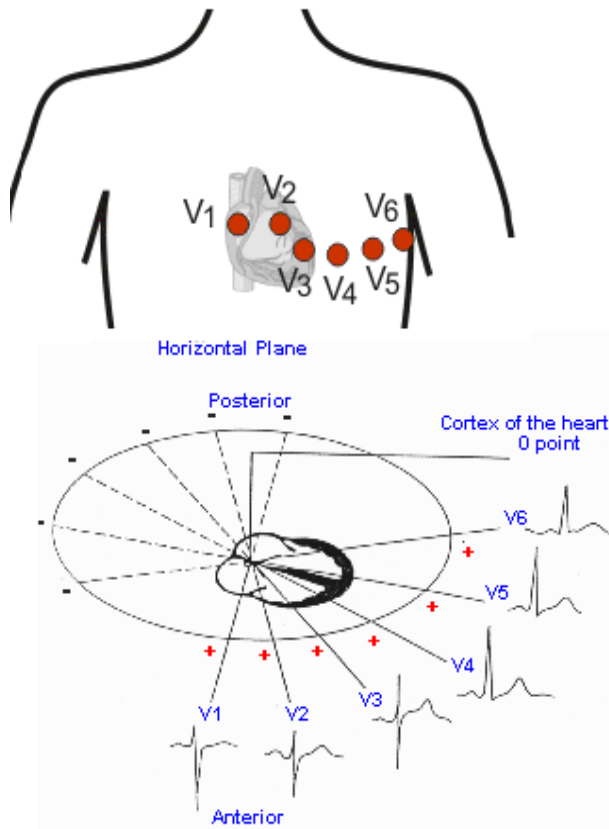


Figure 39 Location of the precordial leads.

V₁ and V₂ are located at the fourth intercostal space on the right and left side of the sternum; V₄ is located in the fifth intercostal space at the midclavicular line; V₃ is located between the points V₂ and V₄; V₅ is at the same horizontal level as V₄ but on the anterior axillary line; V₆ is at the same horizontal level as V₄ but at the midline. Adapted from [27] and [28].

ECG Components

The electrical events of the heart are usually recorded on the ECG as a pattern of a baseline broken by a P wave, a QRS complex, a T wave and a U wave. In addition to the wave components of the ECG, are also defined intervals and segments. An interval is a part of the ECG containing at least one wave and a straight line. A segment is the period of time from the end of one wave to the beginning of the next wave.

In the figure below is shown the principal ECG components and its normal values.

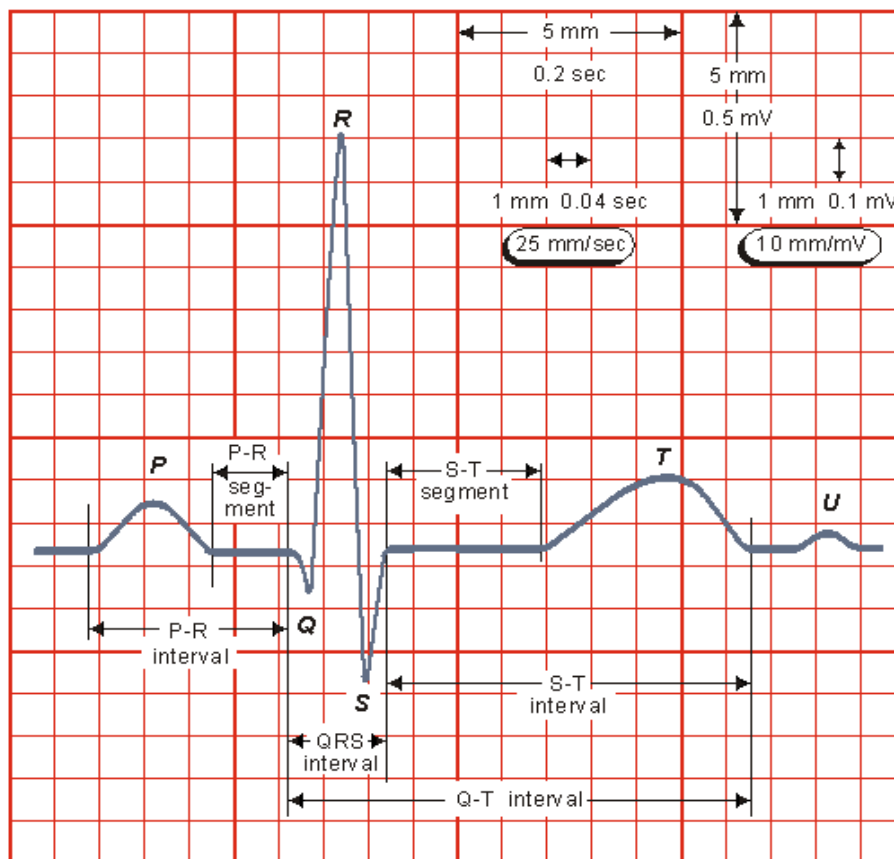


Figure 41 ECG components: waves, segments and intervals.

P wave: Depolarization of atrial muscle as negativity spreads from the SA node toward the ventricles; **QRS complex:** spread of excitation through ventricular myocardium, resulting in depolarization of ventricular muscle. Atrial repolarization is also part of this segment, but the electrical signal is masked by the larger QRS complex; **T wave:** beginning of ventricular relaxation (ventricles repolarization); **U wave:** repolarization of a collection of specialized muscle fibers in the ventricles (Purkinje fibers); **P-R Interval:** time it takes for the impulse sent from the SA node to travel to the ventricles; **P-R segment:** interval between atrial depolarization and ventricular polarization; **S-T Segment:** period during which ventricles are more or less uniformly excited; **Q-T interval:** electrical systole. Sources: [29] and [15].

APPENDIX B

ELECTRONIC CIRCUITS SCHEMATICS

1. Measurement Probe Circuit

The next figure illustrates the schematic of the measurement probe's circuit (first prototype). Only the electronics concerning one of the x-axis accelerometer is shown.

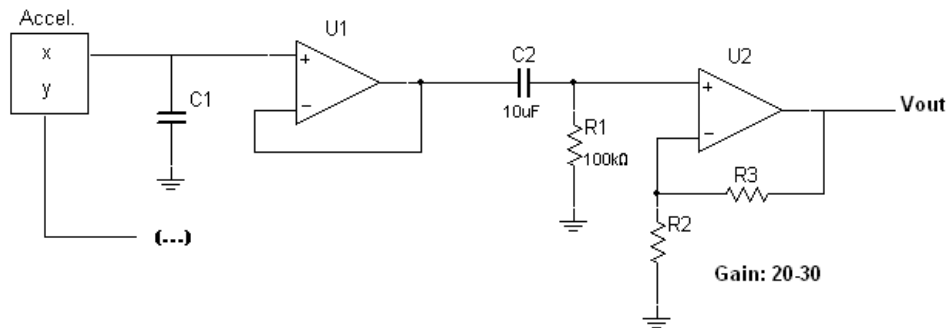


Figure 42 Measurement probe's circuit schematic (first prototype).

2. PZ Single Channel

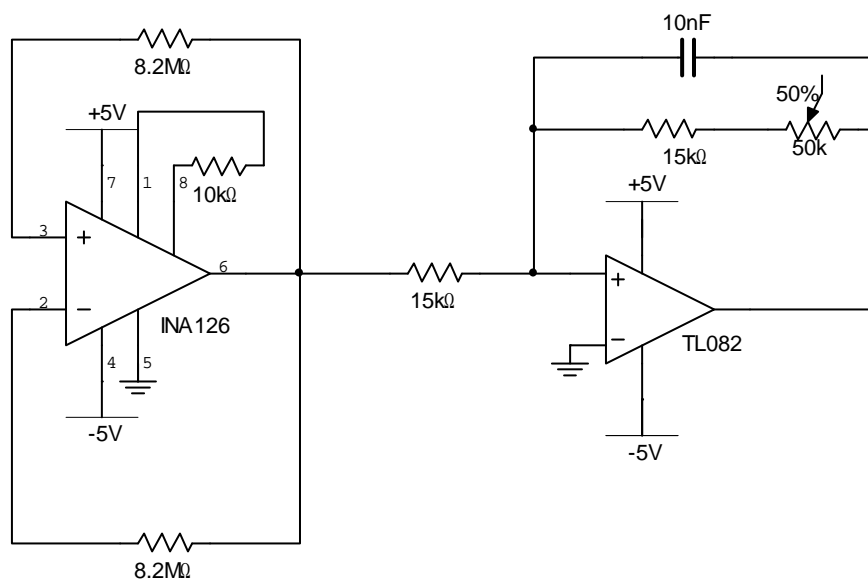


Figure 43 PZ Electronic Circuit of the DAQ Module B.

3. PZs Double Channel

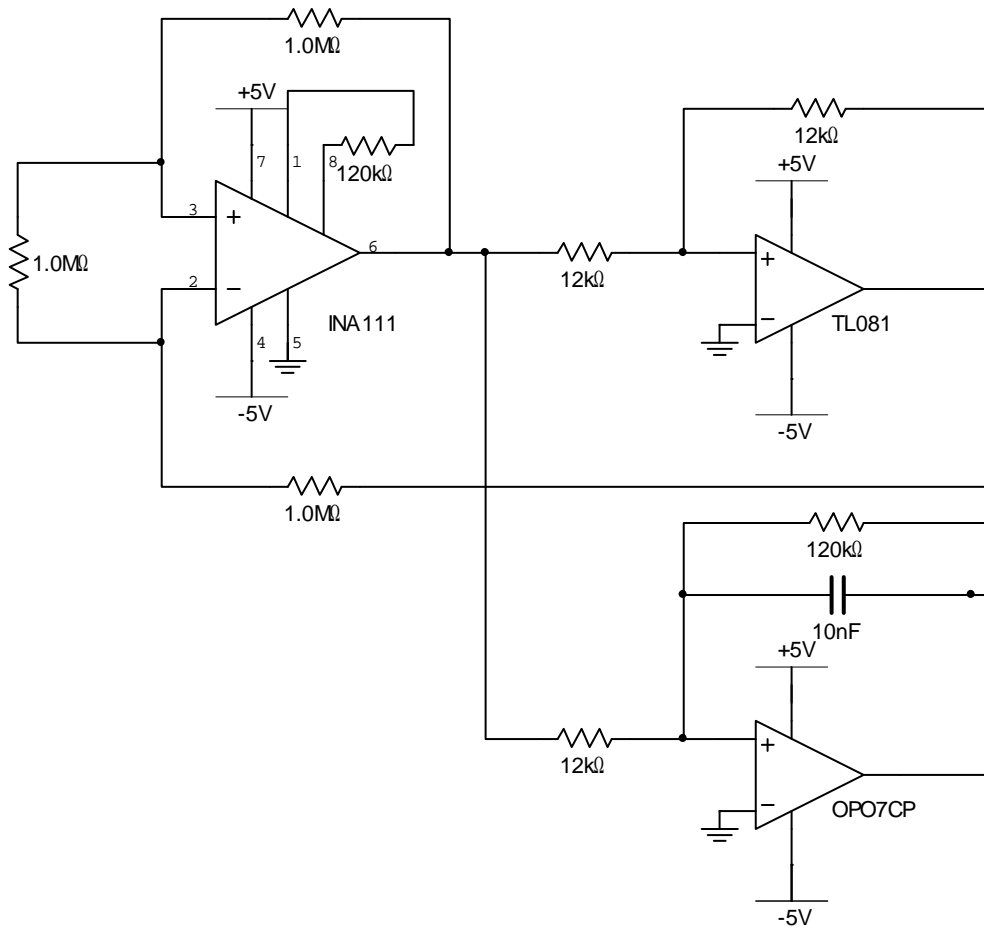


Figure 44 PZ Electronic Circuit of the DAQ Module B.

This architecture is common to both PZs channels.

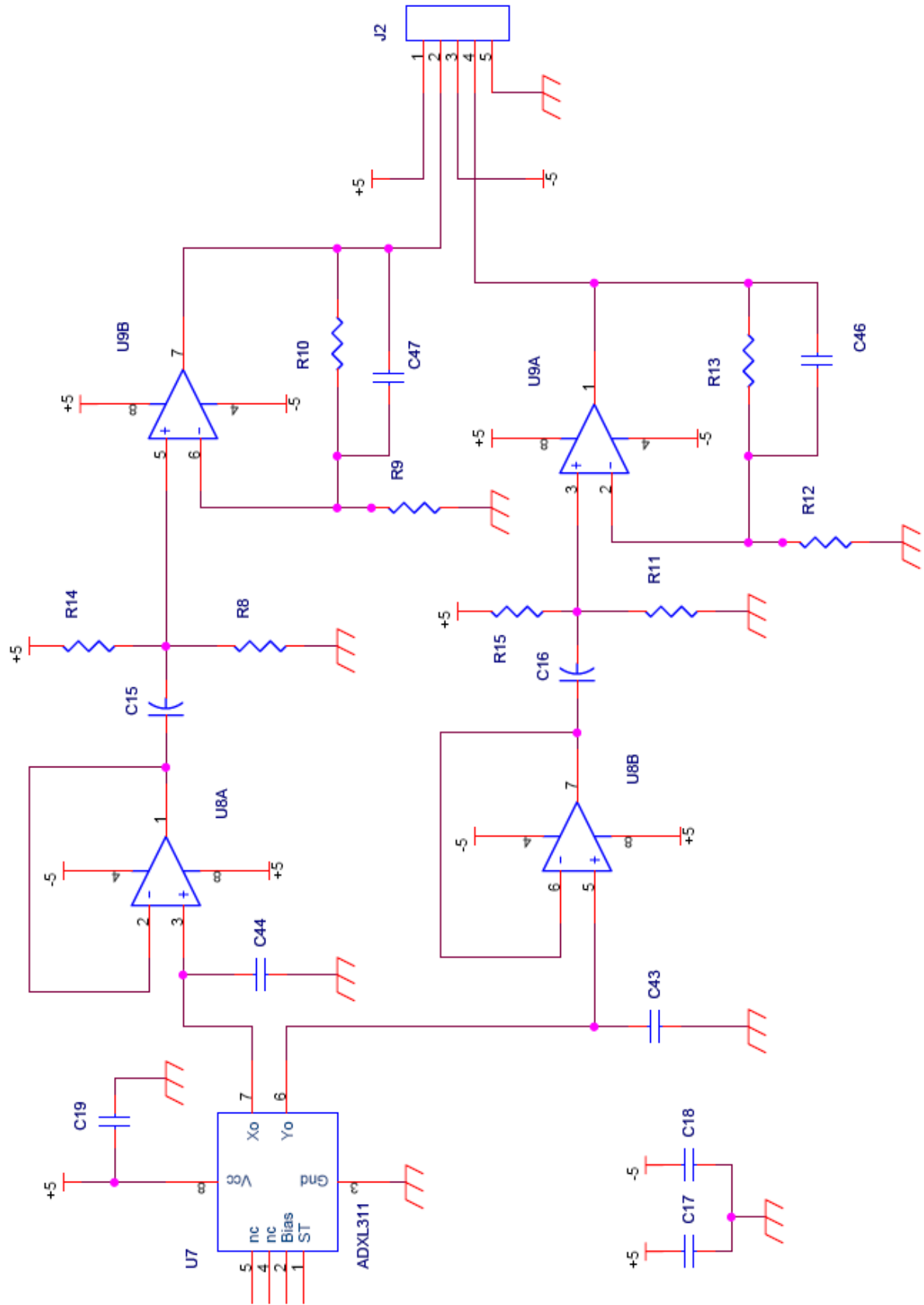


Figure 45 SPL Electronic Circuit Schematic.

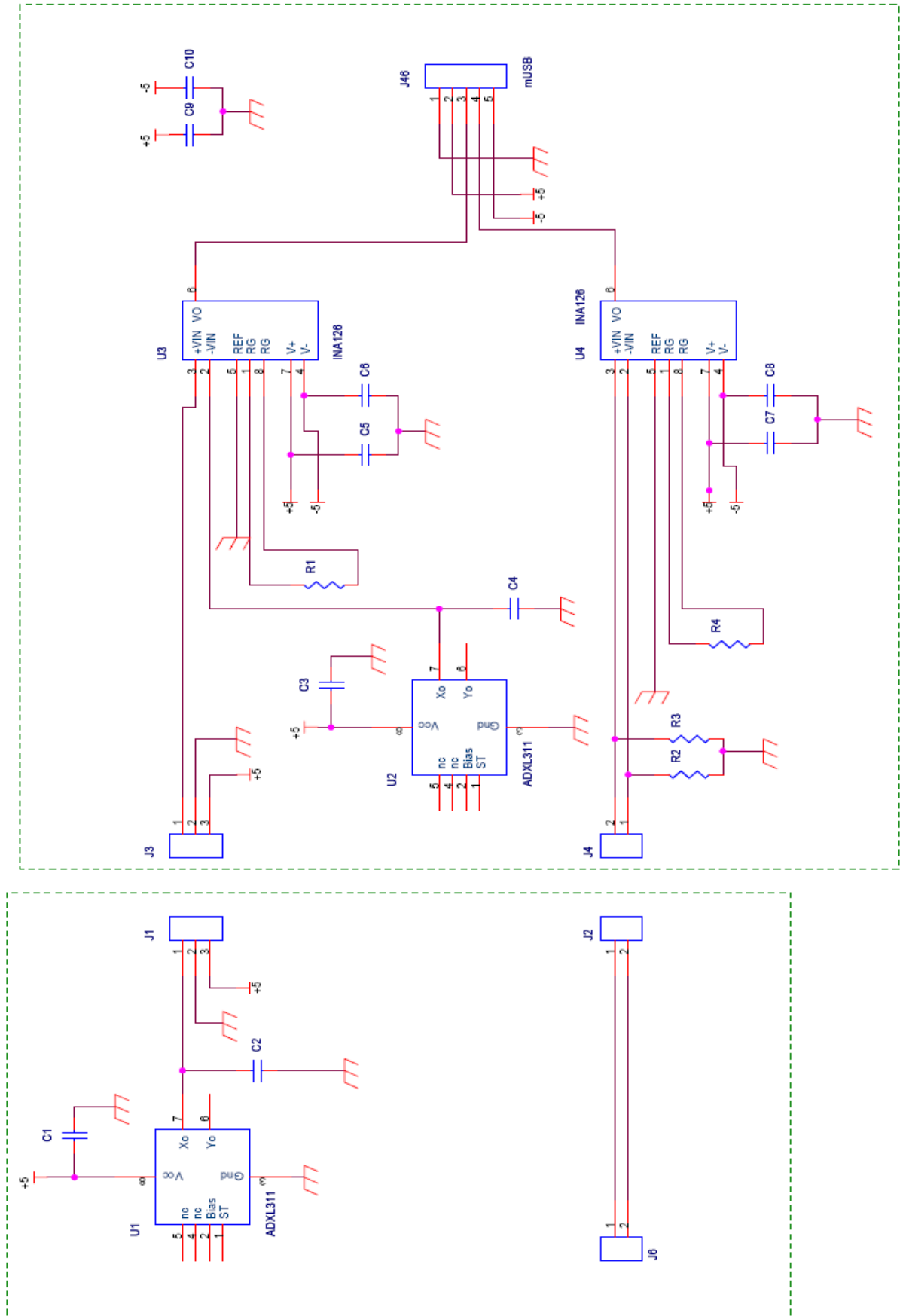


Figure 46 HP Electronic Circuit Schematic.

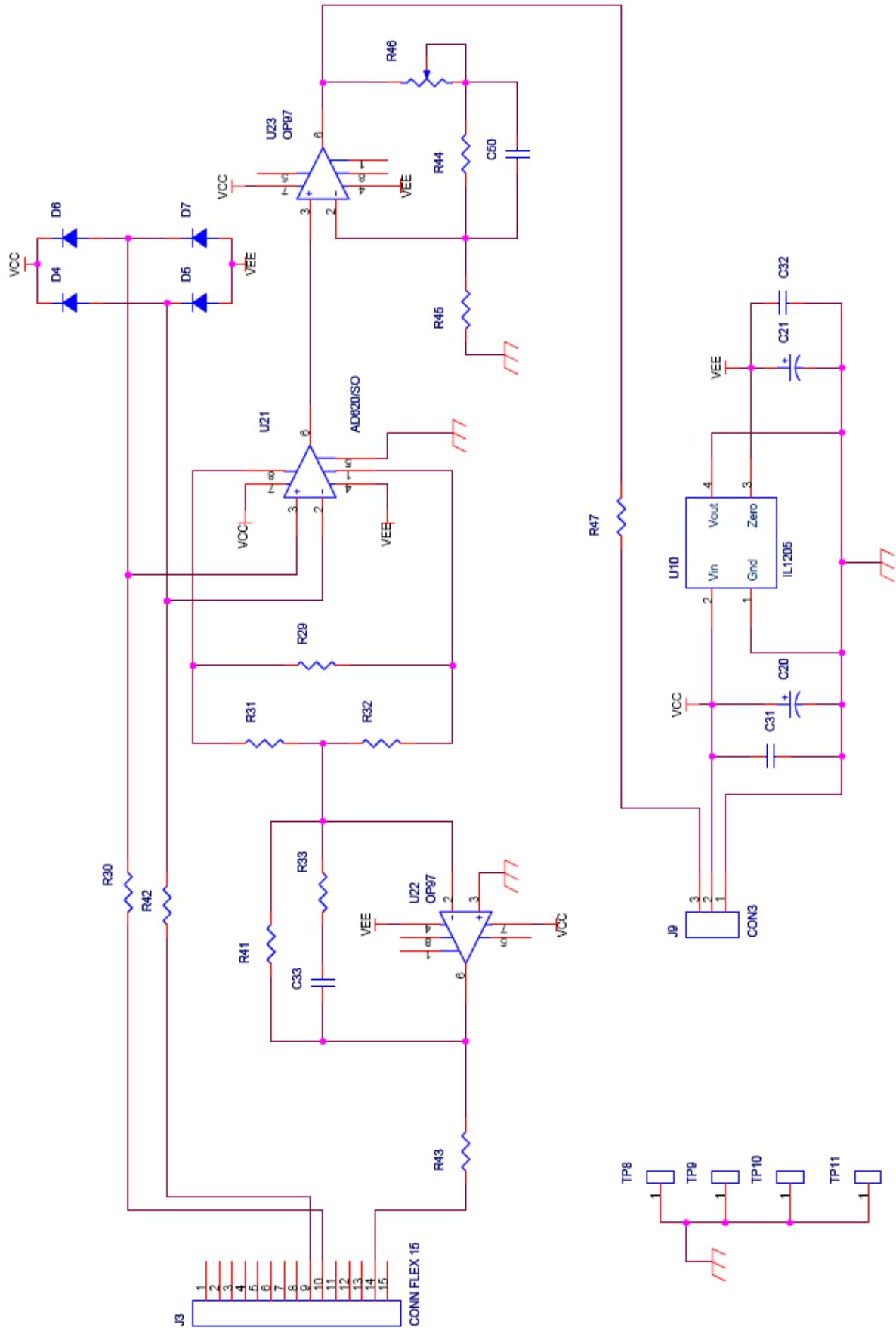


Figure 47 Electrocardiograph Electronic Circuit Schematic.